Ash Chemistry in MSW Incineration Plants: Advanced Characterization and Thermodynamic Considerations, Final Technical Report in EFP Project, J.No 1373/01-0029

Jappe Frandsen, Flemming; Laursen, Karin; Arvelakis, Stelios; Stenseng, Mette; Jørgensen, Tina Lillan; Sørum, Lars; Jensen, Mette K.; Backman, Rainer; Zbogar, Ana; Dam-Johansen, Kim

Publication date:
2004

Document Version
Publisher's PDF, also known as Version of record

Ash Chemistry in MSW Incineration Plants:

Advanced Characterization and Thermodynamic Considerations

Final Technical Report in EFP Project, J. No. 1373/01-0029

Flemming J. Frandsen, Karin Laursen, Stelios Arvelakis, Mette Stenseng, Tina L. Jørgensen, Lars Sørum, Mette K. Jensen, Rainer Backman, Ana Zbogar, and Kim Dam-Johansen.

July 2004

Table of Content:

English Resume:

A number of ash samples where collected at four Danish municipal solid waste incineration (MSWI) plants. Samples of bottom ash/slag, 2^{nd}-3^{rd} pass ashes and ESP/E-filter ash were collected at the plants. The ashes were analyzed by a number of standard chemical analyses, and a number of advanced analytical techniques.

The wet chemical analyses of the different ash fractions revealed that residual ash is formed on the grate by interaction of the main ash forming elements, Al, Ca, Fe and Si. Some of this ash is entrained from the grate and carried with the flue gas along the flue gas duct, where volatile species of K, Na, Pb, Zn, Cl and S starts to condense heterogeneously on the fly ash, thereby causing a dilution of the main ash forming elements. When compared plant-by-plant, the ash chemical analyses showed that the plant with the highest S-content in the fly ash is the one with the most often operational problems in relation to deposition, while a high Cl-content is indicative of a high corrosive potential.

An existing Computer Controlled Scanning Electron Microscopy (CCSEM) algorithm was extended with chemical classes covering Pb- and Zn-rich phases. This has made it possible also to analyze MSW-derived ashes by use of CCSEM.

Representative samples of 2^{nd}-3^{rd} pass and ESP/E-filter ashes from the four plants have been analyzed by Quantitative X-Ray Diffraction (QXRD) analysis. Only a few crystalline phases were identified: KCl, NaCl, $CaSO_4$, SiO_2 and $CaCO_3$ being the main ones. No crystalline phases containing Pb or Zn were identified by QXRD.

A comparison between CCSEM and QXRD revealed the expected surface nature of the CCSEM analysis.

Samples of 2^{nd}-3^{rd} pass and ESP/E-filter ash from the four plants where investigated for melting behavior in the Simultaneous Thermal Analyzer (STA). It was shown that it is possible to quantify the melting behavior of these ashes, and that the melting goes on in two steps (salts followed by silicates/oxides).

The release of heavy metals was investigated as a function of temperature, local stoichiometry and feedstock chemical composition. It was shown that – from a thermodynamic point of view – extreme caution must be taken if trying to affect the heavy metal vaporization by use of additives applied directly to the fuel bed. Thermodynamic modeling was also applied in order to interpret the melting curves generated by analysis of the STA-output.

A complete review of models for different heat transfer mechanisms of importance to deposit temperature profiles and thereby to boiler heat up-take has been performed and submitted as a review paper to an international journal.

Dansk Resumé:

Et antal askeprøver er blevet taget ud på fire danske affalds-fyrede kedler. Prøverne omfatter bundaske/slagge fra risten, 2.-3. træksaske og aske fra ESP/E-filteret på de fire anlæg. Askerne er blevet undersøgt vhja. et antal standard analyseteknikker, såvel som vhja. et antal avancerede analysemetoder.

Vådkemiske analyser af de forskellige askefraktioner har afsløret at der dannes flyveaskepartikler på risten via kemiske interaktioner mellem de askedannende grundstoffer, Al, Ca, Fe og Si. Noget af denne løftes op fra risten af forbrændingsluften og rives med ned igennem kedlen, hvor flygtige forbindelser af K, Na, Pb, Zn, Cl og S, begynder at kondensere heterogent på flyveaskepartiklerne, hvorved hovedelementerne fortyndes i nogen grad. Når askernes kemiske sammensætning sammelignes på tværs af anlæg, viser resultaterne at de anlæg som har højest S-koncentration i flyvesaken også har de hyppigste driftsproblemer i relation til belægningsdannelse. Tilsvarende vil anlæg som producerer Cl-holdig flyveaske have de største problemer i relation til korrosion.

En eksisterende CCSEM algoritme er blevet udvidet med kemiklasser som dækker Pb- og Zn-rige faser, således at det nu også er muligt at analysere flyveasker afledt fra affaldsforbrænding vhja. CCSEM.

Repræsentative prøver af 2.-3. træksaske og ESP/E-filter aske fra de fire aktuelle kedler er blevet analyseret med QXRD. Kun få krystallinske faser er blevet identificeret, inkl. KCl, NaCl, $CaSO_4$, SiO_2 og $CaCO_3$, som de primære. Ingen krystallinske faser rige på Pb og/eller Zn er blevet identificeret vhja. QXRD.

En sammenligning mellem CCSEM og QXRD har afsløret den ventede overfaldnatur af CCSEM.

Prøver af 2.-3. træksaske og ESP/E-filter aske fra de fire kedler er blevet undersøgt for smelteforløb i STA'en. Det er vist at man faktisk kan bestemme smelteforløbet i disse asker vhja. STA, samt at smeltforløbet foregår i to trin (salte og silkater smelter).

Frigivelse af tungmetaller er blevet undersøgt, under antagelse om termodynamisk ligevægt, som funktion af temperatur, redoxforhold og kemsik sammensætning af fødeblandingen. Resultaterne viser at man – set igennem termodynamiske briller – skal være ekstremt forsigtig med brugen af additiver direkte på risten, ihvertfald hvis formålet er at begrænse frigivelse af tundmetaller. Ligevægtsberegninger er også blevet brugt til at fortolke STA-smeltekurver.

En fuldstændig oversigt over modeller for forskellige varmetransportmekanismer af betydning for belægningsdannelse i kedler er gennemført og skrevet sammen i en artikel fremsendt til et international journal.

Chapter 1:

Introduction to Municipal Solid Waste Incineration

By Flemming J. Frandsen

Incineration has been used as a method for processing wastes since the beginning of the last century. Over the last two decades, it has evolved into a widely used, well established technology with reliable modern facilities, operating on a fully commercial basis. Modern MSWI plants are now almost always constructed with energy recovery units.

Waste incineration has many environmental benefits such as:

- Conservation of fossil fuels;
- Reduced use of landfill disposal capacity;
- Stabilization of hazardous compounds, thereby reducing the risk of soil and water pollution associated with waste disposal;
- Re-cycling of nutrients.

Depending on its nature (primarily the heating value), waste can be burned:

- As a principal fuel, with supplementary fuels such as natural gas or fuel oil employed only for the purposes of start-up or maintaining ignition temperature; or
- As a supplementary fuel co-combusted with other wastes or fossil fuels; or
- As a principal or supplementary fuel for direct process purposes, such as cement manufacture.

Incineration is a major disposal option for municipal solid waste in most developed countries, see Table 1-1, though a considerable proportion of the existing deployment in many countries does not have energy recovery.

COUNTRY	*INCINERATION AS PART OF MSW TREATMENT (%)*	*FRACTION WITH ENERGY RECOVERY (%)*
Denmark	65	100 (mostly district heating)
France	42	68
Japan	72	Only few plants
The Netherlands	40	50
Sweden	55	100 (mostly district heating)
USA	16	60
UK	8	Only few plants

Table 1-1: Use of incineration (and energy recovery) for waste disposal in various countries. Source: ISWA Yearbook (1993).

Denmark has the following priorities, for management of municipal solid waste (MSW):

- To reduce waste generation and toxic components in waste,
- to encourage re-use, recycling and energy recovery, and,
- to secure an environmentally safe management of residues

Danish MSW consists of household waste, and waste from the service and trade industry delivered to municipal waste treatment plants or recycling schemes. In 1998, a total of 12,428 million tonnes of MSW was handled as follows (Statistisk Årbog 2000): 58,9 %(w/w) was recycled, 22,1 % was incinerated and 19 % was disposed in landfills.

An average composition of the MSW incinerated in Denmark is shown in Table 1-2.

MSW COMPONENT:	% OF AVERAGE COMPOSITION
Refuse collection	49,7
Bulky refuse	8,5
Garden refuse	0,3
Industrial refuse	31,2
Hazardous refuse	0,04
Hospital refuse	0,1
Miscellaneous other sources	9,8

Table 1-2: Average composition of MSW incinerated in Denmark. Source: Statistisk Årbog 2000.

Combustion of MSW is handled in 32 plants located across the country. All plants are equipped with energy recovery facilities operating with steam temperatures in the range 380 – 450 °C and steam pressures in the range: 35 – 75 bars. The plants cover steam production capacities in the range, and the typical lower heating values of MSW fired in Denmark are in the range: 8 – 13 MJ/kg.

Ash deposition, i.e. slagging and fouling is very complex phenomena which depend on a large number of parameters:

- Release from and transformation in the waste of inorganic metal species, during heat-up, pyrolysis and subsequent char burn-out;
- Flame temperature and quenching during heat recovery (boiler temperature profile);
- Chemical reactions between gaseous, liquid and solid phases (gas-solid/liquid interactions, scavenging);
- Kinetic limits in the gas phase reactions and in particular in aerosol formation;
- Existence of non-equilibrium conditions due to sub-cooling (glass formation), adhesion and detachment/re-entrainment of deposited fly ash particles.

Slagging, fouling and corrosion are also dependent upon a number of design and operational parameters, including:

- Furnace gas exit temperature;
- Furnace design and grate type and operation;
- Tube spacing, orientation and metal surface temperature;

- Air distribution (above/below grate, air nozzle spatial placement and design);
- Steam quality (temperature, pressure, rate of production (kg/s));

Among the influencing operational parameters are:

- Fuel feedstock homogeneity, heating value and size distribution
- Excess air O_2-level
- Flame impingement
- Soot blower operation
- Boiler load

Incombustible parts of the waste fired may not only cause a reduction in the overall plant efficiency due to deposition on heat transfer surfaces, but may also lead to corrosion by fireside deposits of salts, sintered or molten ash. Shortly after the first waste-to-energy plants began to emerge in the mid 1960s, tube depletion was encountered on waterwalls in the furnace and on superheaters. Examination of the problems indicated that tube metal wastage was caused by chlorine, acting independently or in combination with heavy metals like Pb and Zn, and alkalis (Na and K) (Bryers (1996)).

Understanding the formation of troublesome deposits in MSWI plants requires fundamental insight into a number of steps:

- Release of inorganics and formation of ash species (residual ash and aerosols),
- Transport of ash species from bulk gas to heat transfer surfaces,
- Adhesion of ash species to heat transfer surfaces,
- Build-up and consolidation of deposits,
- Break-down and shedding of deposits.

Activities on deposit formation and corrosion in MSWI plants are also going on at the Department of Manufacturing Engineering and Management, Technical University of Denmark. Thus, it was decided to take a step backward in the above description, and focus attention on three main things within this project:

- Ash formation and chemistry,
- Characterization of ashes from MSWI plants, and,
- Thermodynamic evaluation of MSWI plant chemistry,

in close cooperation with the activities at IPL-DTU and other PSO-funded research activities in this area.

This final report covers all issues worked on in the actual project, presented as short summaries. In addition, a paper dealing with most of the characterization work was presented at an international conference on incineration in USA, May 2004. This paper is shown in Appendix A. Appendices B-C, contain two journal papers covering some of the thermodynamic modelling activities carried out within the project.

A complete review on theoretical models for the effect thermal conductivity in a deposit is provided in Appendix D.

Chapter 2:

Plants Considered and Samples Collected

By Flemming J. Frandsen

A number of different ash fractions from different, Danish, MSWI plants were collected, analysed by various analytical methods, and the results were compared. A simplified sketch of a grate-fired MSWI plant is shown on Figure 2-1. Typical gas temperatures in the different boiler sections are shown on the figure.

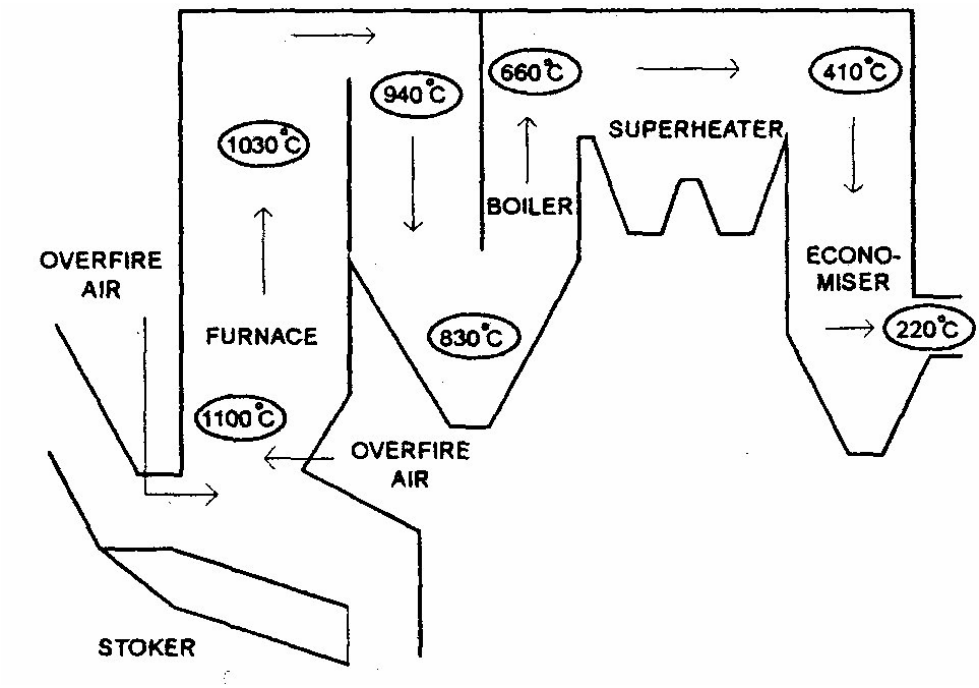

Figure 2-1: Principal sketch of a grate-fired MSWI plant. Typical gas temperatures and different boilers sections are marked on the figure. The slag and bottom ash has been collected in the ash pit at the end of the grate. The 2nd – 3rd pass ash has been collected from the hopper between the 2nd and the 3rd pass of the boiler. And finally, the ESP-ash has been collected from the ESP, which is placed after the Economizer section shown on the sketch.

Three fractions of ash, including 1) slag or bottom ash from the furnace, 2) fly ash from the ash hopper between the 2nd and the 3rd pass, and, 3) fly ash from the final particulate removal device in the flue gas duct, eg. an electrostatic precipitator, was collected at a significant number of MSWI-fired plants all over Denmark, see Figure 2-2.

In order to make an overview of the results easy, and secondly, in order not to use too many money on analyses before a consistent set of ash characterization methods have been developed and tested, four different Danish MSWI plants: Hjørring, KARA,

Nordforbrænding and Sønderborg, was selected as prime focus MSWI plants. Thus, it is primarily results from analyses of ashes from those four plants that will be outlined in this report.

Figure 2-2: The MSWI plants originally involved in this project. In order to process a reasonable amount of analyses, four of the plants were chosen as prime focus plants.

For the four prime focus MSWI plants, major configuration and plant operational data are provided in Table 2-1 and 2-2.

It is seen from Tables 2-1 and 2-2 that the plants picked for further investigation are of similar configuration, operation and size. Nevertheless, they experience quite different problems in relation to their operation, reflecting basically the effect of the fuels fired.

PLANT	ESTAB-LISHED	RATING T/H	FURNACE TYPE	BOILER TYPE	FLUE GAS CLEANING
Hjørring	1998	12	Moveable (Krüger)	Warm water (BWE)	Wet (ABB)
KARA	1999	20	Moveable (Alstom)	Steam (BWE/FLS)	ESP/Wet/FF (ABB)
Nord-forbrænding	1991	11	Moveable (B&S)	Steam (Ålborg Boilers)	Semi-dry/ESP (FLS)
Sønderborg	1996	8	Moveable (Krüger)	Steam (BWE)	Wet (ABB)

Table 2-1: Basic boiler data for the prime focus boilers considered in this project. B&S: Bruun & Sørensen. Source: ISWA (2002)

PLANT	FLUE GAS TEMP. (°C)	STEAM TEMP. (°C)	STEAM PRESSURE (BAR)	HOUSEHOLD WASTE (%)	INDUSTRIAL WASTE (%)
Hjørring	60	400	48	60	39
KARA	120	440	40	48	46
Nord-forbrænding	150	425	59	60	40
Sønderborg	65	420	60	72	28

Table 2-2: Basic boiler data for the prime focus boilers considered in this project. B&S: Bruun & Sørensen. Source: ISWA (2002)

Chapter 3:

Mapping of Ash Chemistry in MSWI Plants

By Flemming J. Frandsen

The fate and partitioning of the inorganic elements during the incineration process are highly dependent on their physicochemical properties (IAWG, 1997):

- The non-volatile (or lithophilic) elements are generally considered tightly fixed in the waste fuel, and they will primarily remain in the condensed phase during incineration. Consequently, the major part of these elements will be present in the bottom ash fraction. These elements have boiling points far above 1500°C. The most abundant lithophilic elements in MSWI are Si, Al, Fe and Ca. They form very stable oxides, silicates and aluminosilicates, which constitute the major fraction of a bottom ash.
- The volatile (atmosphilic) elements, which include elements forming acid gases i.e. halogens, sulfur, and alkali and trace metals, are partly or fully volatilized in the furnace. When the flue gas temperature decreases downstream of the furnace, the volatilized elements may undergo homogeneous nucleation reactions due to supersaturation, or they may condense heterogeneously on the surface of fly ash particles or on heat transfer surfaces. The major part of the volatile elements are subsequently cached by the flue gas cleaning system, the rest are discharged with the flue gases.

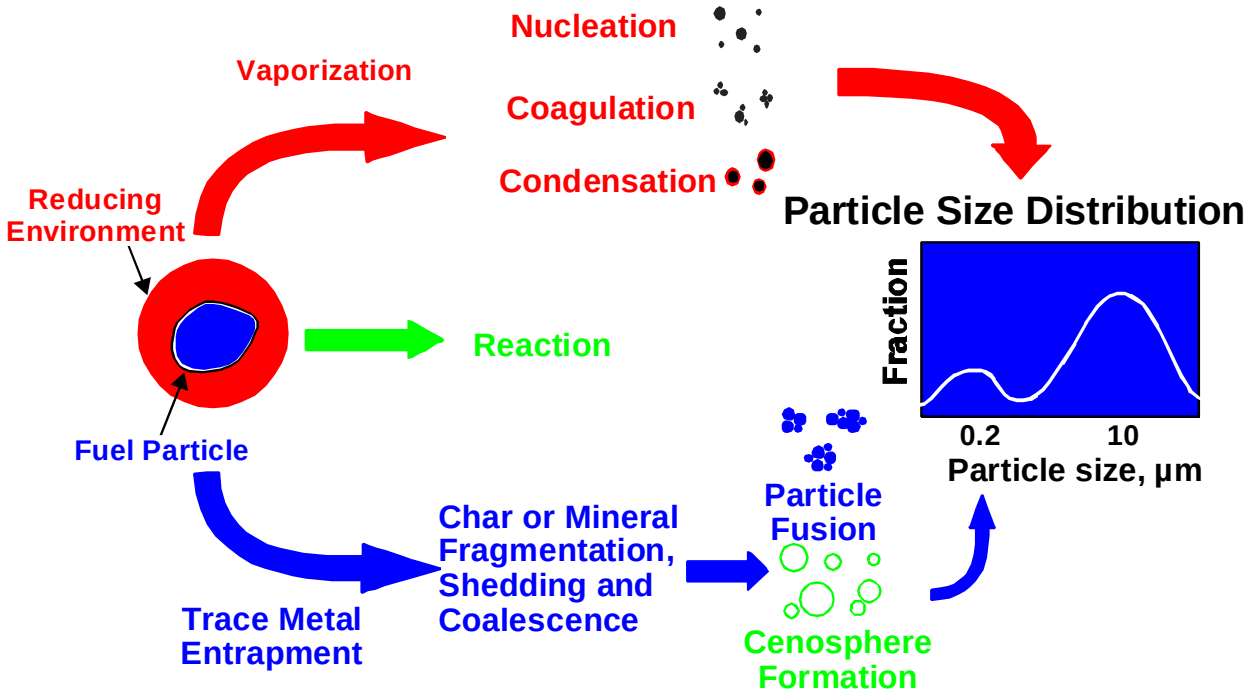

Figure 3-1: Main routes of ash formation in solid fuel thermal conversion.

A schematic diagram of ash formation is shown in Figure 3-1.

The ashes collected at the four MSWI plants were analyzed for their bulk chemical composition by use of ICP-OES technique. In Figure 3-2, a comparison of the molar fraction of Ca and Zn in the slag, the 2nd-3rd pass ash and the ESP/E-filter ash, is shown.

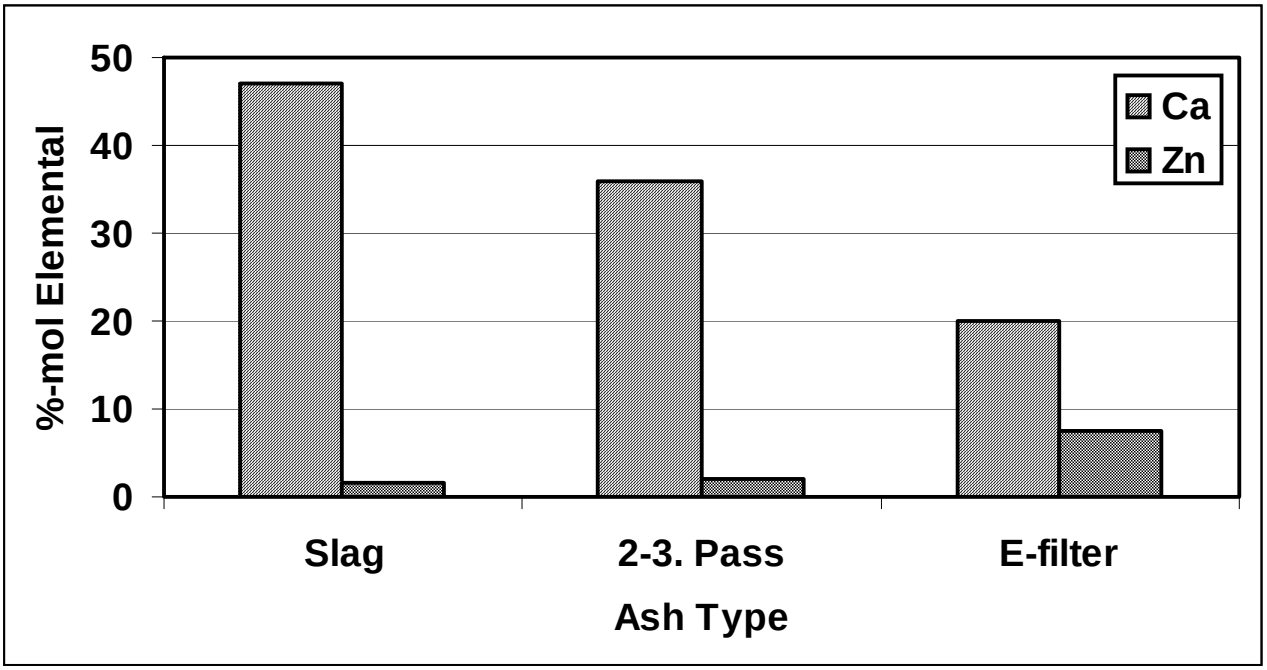

Figure 3-2: The concentration of Ca and Zn, shown as %-mol Ca respectively Zn in the three different ash fractions collected at the Hjørring MSWI Plant.

It is seen in Figure 3-2, that the slag and the ash from the 2nd-3rd pass have a rather high content of Ca. In the ESP/E-filter ash a somewhat lower concentration of Ca is measured. A similar behaviour is observed for the elements Al, Fe and Si, who all are diluted when going from the slag/bottom ash in the furnace to the ESP/E-filter ash.

It is also seen on the figure that the slag and the ash from the 2nd-3rd pass have a rather low content of Zn. In the ESP-ash (or E-filter ash) a somewhat higher concentration of Zn is measured, ie. the exact opposite behaviour to Ca is observed for Zn. A similar behaviour is observed for the elements K, Na, Pb, Cl, and S, who all are enriched when going from the slag/bottom ash in the furnace to the ESP/E-filter ash. Thus, condensation of volatile elements like Na, K, Pb, S, Cl and Zn causes a dilution of the content of non-volatile elements like Si, Al, Fe and Ca in the e-filter ash.

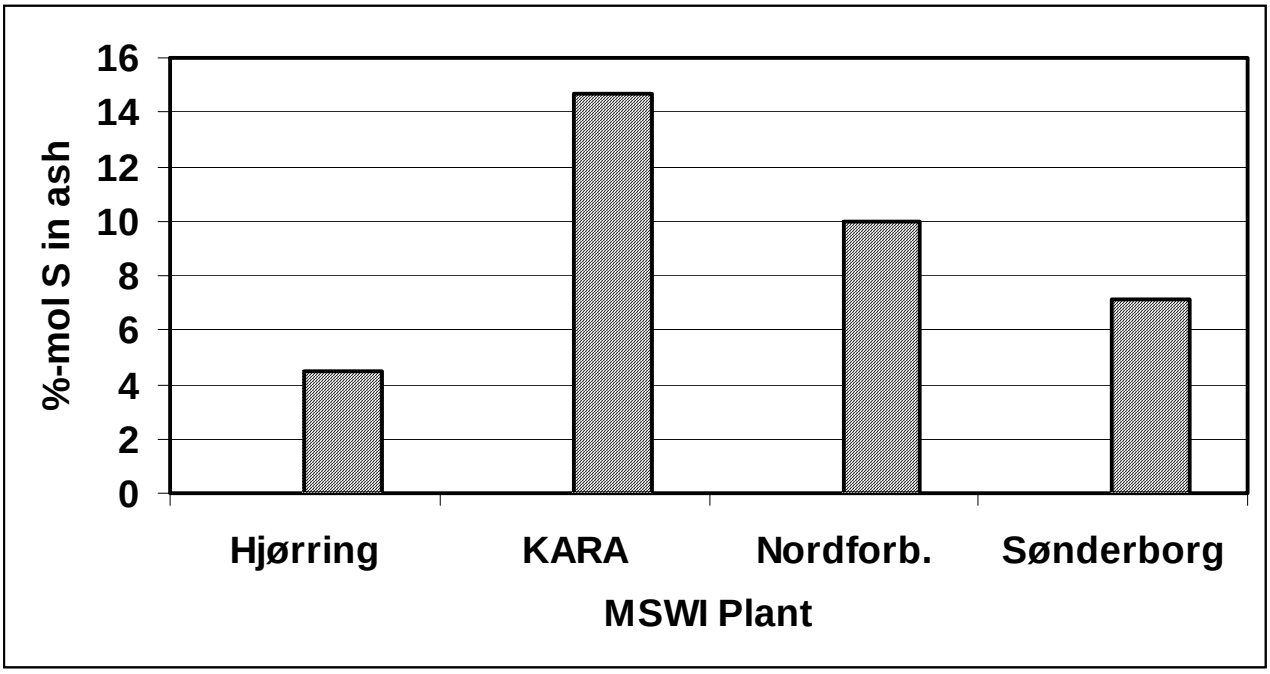

Figure 3-3: Comparison of the concentration of S, shown as %-mol S in the ash, in the ESP/E-filter ash collected at the four different plants.

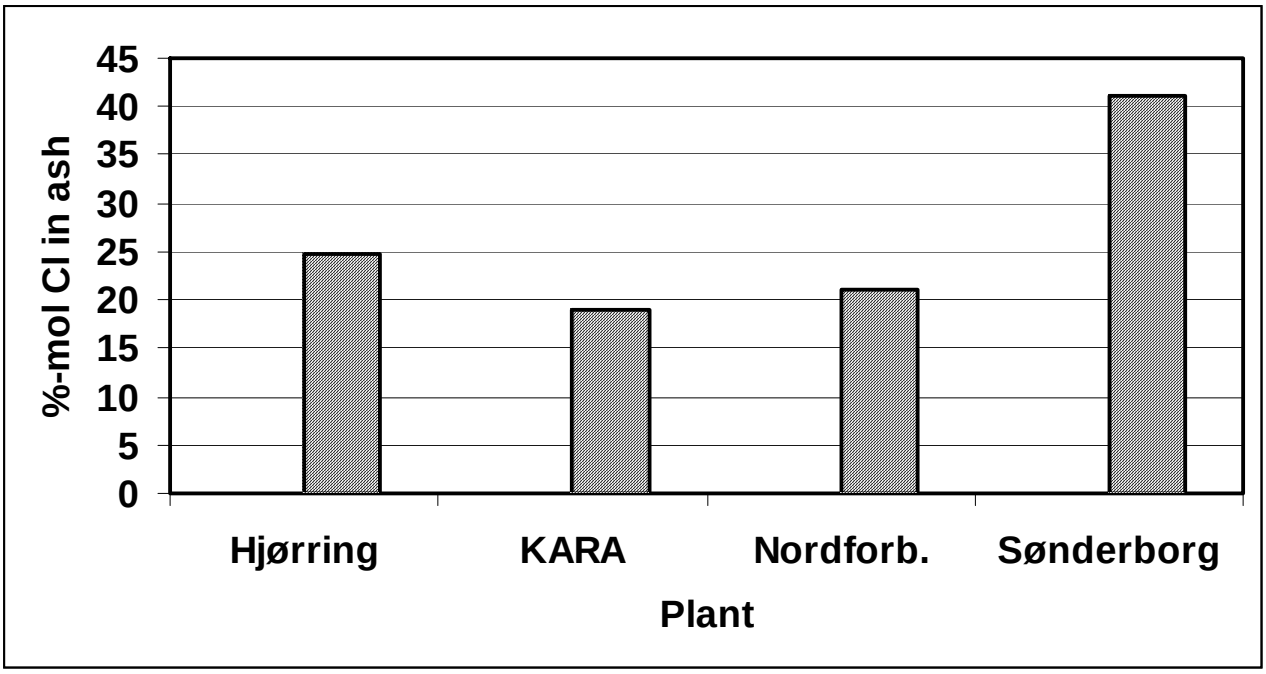

Figure 3-4: Comparison of the concentration of Cl, shown as %-mol Cl in the ash, in the ESP/E-filter ash collected at the four different plants.

An interesting feature shows up when comparing the chemistry profiles for the four MSWI plants considered. In Figure 3-3, a comparison of the concentration of S, i.e. %-mol S in the ESP/E-filter ashes, is shown. It is seen that the KARA MSWI plant has the highest

level of S in the ESP/E-filter ash, which correlates with the fact that this plant, when these ashes were collected experienced some problems with deposit formation in the empty 2nd-3rd pass.

Similarly, in Figure 3-4, a comparison of the concentration of Cl, in the ESP/E-filter ash, is shown. From these figures it becomes evident, that the Sønderborg plant has the highest molar concentration of Cl, which is interesting in relation to the corrosion problems that this plant is experiencing from time to another.

Finally, in Figure 3-5, a comparison of the concentration of Zn, in the ESP/E-filter ash is shown. It is seen that the KARA, respectively, the Sønderborg MSWI plants have the highest concentration of Zn in the ESP/E-filter ash. This seems to indicate that zinc may play a role in mobilizing S and Cl, thereby causing deposition respectively corrosion problems in MSWI plants.

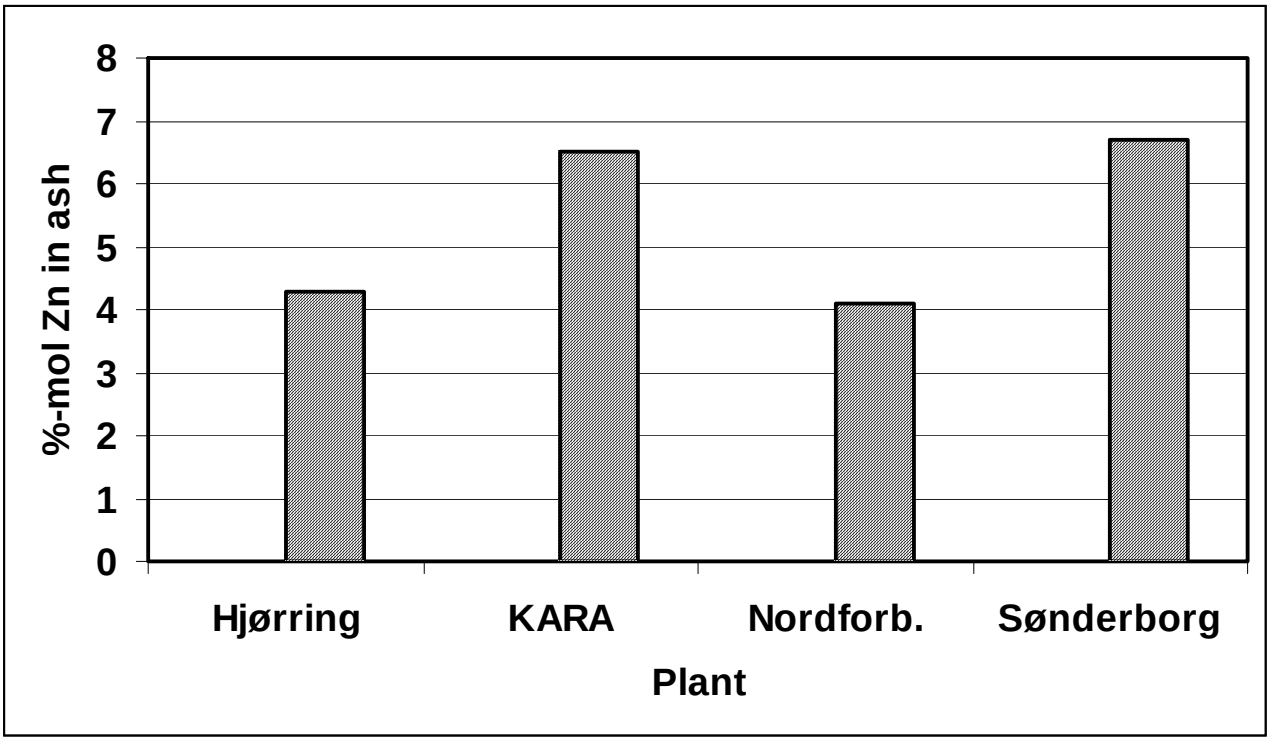

Figure 3-5: Comparison of the concentration of Zn, shown as %-mol Zn in the ash, in the ESP/E-filter ash collected at the four different plants.

Chapter 4:

Advanced Characterization Methods

By Flemming J. Frandsen, Karin Laursen, and Stelios Arvelakis

In order to identify and characterize the ashes formed during thermal conversion of waste, a number of properties and characteristics need to be measured, including, physical, chemical and leaching properties of the ashes (IAWG(1997)). The physical testing of ash should include the following parameters: [1)] visual observations, [2)] particle size distribution, [3)] bulk density, dry density and specific gravity, and, finally, [4)] moisture content and absorption capacity. The chemical testing should include the following parameters: [1)] loss on ignition, [2)] mineralogical composition, [3)] pH and acid neutralization capacity, and, finally, [4)] the total elemental composition and chemical speciation. Finally, the leaching testing should include the following parameters: [1)] the total ability of elements or species for leaching, [2)] the solubility of elements or species as a function of pH, [3)] the effect of contaminant release as a function of the liquid-to-solid ratio, [4)] the alkalinity of the residue, [5)] the presence of complex agents, and, [6)] the primary anions and cations being present in the leachate.

In this paper, the prime focus is on the chemical speciation of MSWI ash. There are different analytical methods available for examination of solid phase chemical speciation of MSWI residues (IAWG (1997)):

- Transmitted Light Microscopy (TLM): Morphology of small ash particles.
- Scanning Electron Microscopy (SEM): Morphology of ash particles.
- Scanning Electron Microscopy - Energy/Wavelength Dispersive X-Ray Analysis (SEM-EDX/WDX): Pseudo-elemental composition
- Scanning Tunnelling Microscopy (STM): Micro topography of a surface down at the atomic layer.
- Computer Controlled Scanning Electron Microscopy (CCSEM): Size distribution and chemical classification of a powdery sample.
- Quantitative X-Ray powder Diffraction (QXRD): Mineralogy of crystalline phases.
- Auger Electron Spectroscopy (AES): Elemental composition on the sample surface.
- X-Ray Flourescence (XRF): Elemental composition
- X-Ray Photoelectron Spectroscopy (XPS): Elemental composition on the sample surface.
- Time-of-Flight Secondary Ion Mass Spectrometry (TOF-SIMS): Surface chemical composition
- Simultaneous Thermal Analysis (STA): Investigation of the melting of ashes.

In the present project, we have applied SEM-EDX/CCSEM, XRD and STA analysis for characterizing the chemistry and melting behaviour of MSWI ashes.

4.1. CCSEM Analysis

Computer Controlled Scanning Electron Microscopy (CCSEM) was used to determine the size distribution and semi-quantitative composition of the inorganic grains in the 2^{nd}-3^{rd} pass and ESP/E-filter ashes.

Prior to analysis, the ash sample was mounted in epoxy, cross sectioned, and polished in water-free glycerin, in order to avoid solubility of salts being present in the sample. The polished surface is coated with a thin C-layer to make it electron conducting. During the analysis, a number of random areas were selected on the sample at magnifications of 25x, 100x and 500x. During scanning of each area, the signal from the backscattered electrons was transformed into a binary, digital image, where inorganic particles of the fly ash appear white, while the rest of the image is black. On each identified white particle, an EDX-analysis is used to detect the chemical composition of the particle with respect to the following elements: Na, Mg, Al, Si, P, S, Cl, K, Ca, Ti, Cr, Mn, Fe, Ni, Cu, Ce, Zn, Sn and Pb. In addition, the area of the particle was determined by multiplying the number of pixels covered by the particle, by the individual pixel area. The semi-quantitative chemical compositions of the particles were used to classify the particles into mineral/chemical categories. Based on the cross sectional area of the particles, and the assumption that the particles are spherical, their diameter is calculated. The diameter is used to separate the particles into size bins. Thus, the output from the CCSEM analysis consists of combined information on the size distribution and the chemical composition of the sample. An important thing to realize about the chemical categorization in the CCSEM analysis is that some of the chemical categories posses mineral names, e.g. calcite. A particle categorized by the CCSEM as calcite is not chemically pure $CaCO_3$ (calcite), but something that chemically looks like calcite. This is the semi-quantitative nature of the CCSEM analysis. In this paper, CCSEM category names will be shown in *italic* (Laursen (1997)).

The categories applied, depend upon the chemistry of the actual ash sample. The definition of the original set of CCSEM chemical categories, developed for analysis of coal-derived fly ash, is listed in Laursen (1997). Sørensen (1999) extended the CCSEM classification scheme, in order to include also chemical compositions common in straw-derived fly ash particles. Fly ashes from waste incineration usually contain significant amounts of Zn and Pb. Thus, we decided to extend the CCSEM classification scheme to include also fly ash from MSWI plants. For that purpose, the new classes defined in Table 4-1, were added to the scheme.

The CCSEM analyses of ash from 2^{nd}-3^{rd} pass respectively from the ESP/E-filter are provided in Table 4-2. The 2^{nd}-3^{rd} pass ashes are rich in silicate bearing phases like *Ca silicate*, *Ca-Al silicate*, *K-Ca silicate* and *quartz*, while the ESP/E-filter ashes reveal signs of condensation of flame volatile species. CCSEM chemical categories like *Ca-Pb rich* and *gypsum + ZnCl2*, indicates condensation of Pb- and Zn-species on the surface of Ca-rich particles of e.g. gypsum or calcite.

CCSEM Chemical Category	*Definition of the Category (%(w/w))*
$ZnCl_2$	Zn>=30; Cl>=30; (Zn+Cl+Ca)>=70
Gypsum+$ZnCl_2$	Si<10; S>20; Ca>20; (Ca+S)<80; Zn>=5; Cl>=5; Ti<10; P<=5
$ZnSO_4$	Zn>=30; S>=30; (Zn+S+Ca)>=80
Zn-Ca silicate	Si>=20; Si<=80; Ca>=15; Zn>=15; Al<=20
Zn-Ca rich	Si<=20, (Zn+Ca)>=40; Ca>=15; Zn>=15; Al<=20
$PbCl_2$	Pb>=25; Cl>=15; Si<20; Zn<15; P<15; S<15
Pb-rich chloride	Pb>=10; Cl>=15; (Pb+K+Na+Cl)>=70
Ca-Pb rich	Ca>=20; Si<20; Pb>=5; Zn<15; P<15; S<15; Cl<15
Pb-rich	Ca<20, Si<20, Pb>=10; Zn<20; P<15; S<15; Cl<15

Table 4-1: New chemical categories defined in order to perform CCSEM analyses on fly ashes derived from waste incineration.

CCSEM Category	*2^{nd}-3^{rd} Pass Ash*	*Electro Filter Ash*
Ca silicate	5.36	
Ca-Al silicate	6.77	
Calcite	5.47	
Ca-rich	2.19	
Gypsum	2.79	4.83
K-Ca silicate	20.39	13.72
Quartz	8.83	
Si-rich	2.39	2.71
Ca-Pb rich		2.80
Gypsum + ZnCl2		2.13
unclassified chloride		12.35
unclassified silicate	17.58	7.87
Unclassified	15.26	40.39

Table 4-2: CCSEM analyses of 2^{nd}-3^{rd} pass ashes and electro filter ashes from the Hjørring MSWI Plant. Only phases constituting more than 2 %(w/w) of the ash are shown.

4.2. QXRD Analysis

The three-dimensional structure of non-amorphous materials, such as salts, is defined by regular, repeating planes of atoms forming a crystal lattice. When a focused X-ray beam interacts with these planes of atoms, a part of the beam is transmitted, a part is absorbed by the sample, a part is scattered, and a part is diffracted. X-rays are diffracted by each salt differently, depending on what atoms make up the crystal lattice of the salt or crystal, and how these atoms are arranged.

When an X-ray beam hits a sample and is diffracted, the distanced between the plans of the atoms that constitute the sample can be estimated by applying Braggs law, which is:

$$n \cdot \lambda = 2 \cdot d \cdot \sin[\theta]$$

where the integer n is the order of the diffracted beam, λ is the wavelength of the incident X-ray beam, d is the distance between the planes of atoms (the d-spacing), and θ is the angle of incidence of the X-ray beam. Since λ is known and θ can be measured, we can calculate the d-spacing. The characteristic set of d-spacings generated in a typical X-ray scan provides a unique 'fingerprint' of the salt or mineral species being present in the sample. When properly interpreted, by comparison with standard reference patterns and measurements, this 'fingerprint' allows for identification of the material.

In this study, powder Quantitative X-Ray Diffraction (QXRD) was used to determine the amount of crystalline phases and amorphous material in the 2^{nd}-3^{rd} pass and ESP/E-filter ashes. The as-received ash samples were pulverized in a laboratory-scale ball-mill. In order to quantify the amount of amorphous material, each sample was mixed with 50 %(w/w) corundum (α-Al_2O_3). Data were collected on a Siemens D5005 Bragg-Brentano diffractometer using CuKα radiation operating at 40 kV and 40 mA. The samples were analyzed in the 2-θ - range: 5 – 80 °, with a step-size of 0.04° and a counting time of 5 sec per step. Phase identification were conducted using the search match program EVA (Bruker DiffracPlus, Version 2.0) supported by the powder diffraction data file (PDF-2, Release 2001). Quantification of the crystalline and amorphous material was conducted using the TOPAS Program (Bruker DiffracPlus, Version 2.0) and the fundamental parameters approach (FPA), see Cheary and Coelho (1992).

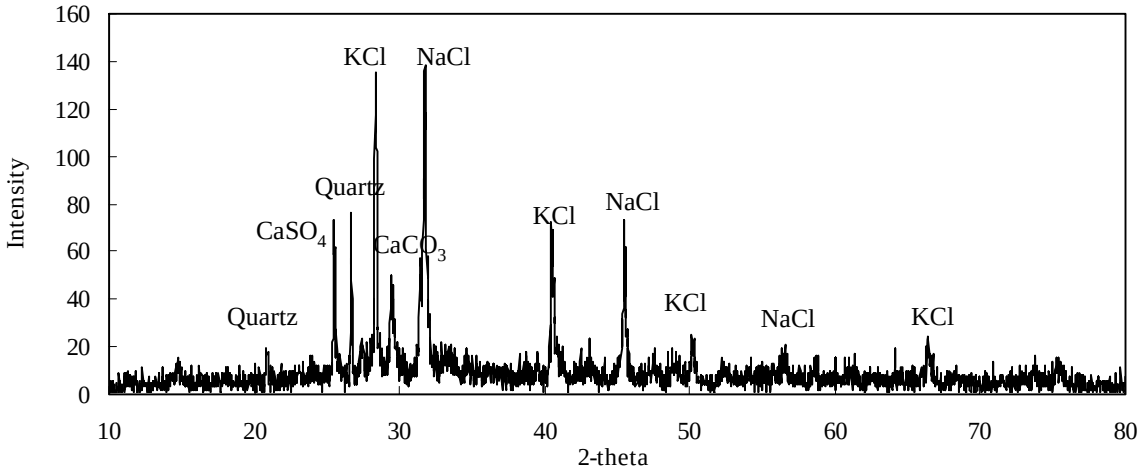

Figure 4-1: QXRD-diagram for ESP/E-filter ash from the Hjørring MSWI Plant.

A QXRD-diagram for the ESP/E-filter ash from the Hjørring MSWI plant is shown in Figure 4-1. It is seen that the following phases are identified on the diagram: Quartz (SiO_2), Halite (NaCl), Sylvite (KCl), Calcium sulphate ($CaSO_4$), Calcite ($CaCO_3$), and, Calcium sulfite hydrate ($CaSO_3.0.5H_2O$). The same phases are identified when analysing the ESP/E-filter ash from the other three plants. In the 2^{nd}-3^{rd} pass ash from the four plants only Quartz (SiO_2) is identified by QXRD.

In Table 4-3, a comparison between the QXRD-analyses and the CCSEM analyses performed is made for the ESP/E-filter ash from the four plants. It is seen that there are certain discrepancies between QXRD-based salt chemistry and CCSEM-based salt chemistry. Because CCSEM does not distinguish between crystalline and amorphous phases, discrepancies between CCSEM and QXRD analyses are to be expected for these ashes, as they contain a large proportion of amorphous material. In addition, it is obvious from the fraction of ash in the 'unknown'-categories of the CCSEM, that a certain improvement of the chemistry classification within CCSEM is still needed.

QXRD		*Hjørring*	*Nordforbr.*	*KARA*	*SKVV*
Quartz	SiO_2	4.28	1.81	4.13	1.46
Calcite	$CaCO_3$	7.44	9	3.47	6.11
Anhydrite	$CaSO_4$	10.38	13.46	15.57	13.65
Sylvine	KCl	7.92	6.7	2.27	8.08
Halite	NaCl	12.19	9.26	7.89	10.89
Amorphous (glass)		58.24	60.03	66.86	59.95
Total		100.45	100.26	100.19	100.14
CCSEM					
Alumina					
Ca silicate		1	1	1	
Ca-Al silicate			4		1
Calcite			2		
Ca-Pb rich		2	6	3	3
Ca-rich			2		
Ca-Si rich			1		
Ca-Ti rich					
Dolomite					
Gypsum		1	2	5	5
Gypsum + ZnCl2				2	3
Illite				1	
K-Ca silicate		7	7	14	10
Na-Al silicate					
NaCl					
NaCl + KCl					
Quartz		1		2	
Rutile					
Si-rich		1	1	3	1
Unclassified		30	39	40	40
Unclassified chlorine		47	23	12	7
Unclassified phosphate					
Unclassified silicate		2	4	8	5
Unclassified sulphate				2	
Zn-Ca rich					16
Total		93	94	93	92

Table 4-3: Comparison of XRD- and CCSEM-analyses of ESP/E-filter ashes from the four MSWI plants considered. All data are on a %(w/w)-base.

Chapter 5:

Melt Quantification in MSWI Ashes

By Flemming J. Frandsen, Mette Stenseng, Tina Jørgensen, Stelios Arvelakis

Thermal analysis methods may be defined as a group of techniques in which a physical property of a substance and/or its reaction products is measured as a function of temperature whilst the substance is subjected to a controlled temperature programme. Different physical properties may be measured: thermogravimetry (TG), derivative thermogravimetry (DTG), differential thermal analysis (DTA), and differential scanning calorimetry (DSC).

Thus, thermal analysis techniques can used to characterise the change in material properties as a function of temperature. The results presented in this paper were obtained at the Department of Chemical Engineering, Technical University of Denmark, using a NETZSCH STA409. Using STA, the sample and an inert reference material are placed in a furnace and subjected to a desired heating programme, typically heating from 20 to 1300 °C, with a heating rate of 10°C/min. The analysis implies continuous measurement of the sample weight (TG) and the sample temperature (DTA or DSC) during heat-up. In this technique, the weight measurement reveals any mass changes occurring in the sample. By comparing the sample temperature to that of the inert reference material any heat-producing or -consuming chemical or physical processes taking place in the sample may be detected. The heat evolved or consumed is quantified by integrating the area below the peak in the DSC-curve and multiplication with an apparatus and temperature dependent factor.

In Figure 5-1, the output from an STA-analysis of the ESP/E-filter ash from the Hjørring MSWI plant is shown. All signals are provided, including the corrected baseline (shown in green colour).

The procedure for ash melt quantification, developed by Hansen et al. (1999), is based on the assumption that when dealing with ash samples, only two types of transformations accompanied by heat effects occur: evaporation and melting. This means that chemical reactions and crystallization processes are not considered. Evaporation can be easily identified, since a weight loss accompanies the process and the weight loss is quantifiable by means of the balance. The temperature at which evaporation takes place may allow the identification of the compounds that evaporates. When this is possible, and the exact evaporation enthalpy of the evaporating compound is known, the contribution of the evaporation enthalpy can be subtracted from the overall enthalpy.

Verification of the following conditions is important for the calculation of the melting curve of an ash sample:

- The occurrence of other processes accompanied by heat effects at zero weight change, namely chemical reactions and glass devitrification can be excluded.
- Melting is complete at the end of the heat treatment. This may not be immediately evident. Also, a *post mortem* SEM analysis may have difficulties in confirming it. In fact, for glassy substances, crystallization can appear during cool-down even at relatively fast cooling rates. Crystals present in the ash after the thermal treatment may therefore be indication of an uncompleted melting of the ash, but they may also be generated during the cooling process.

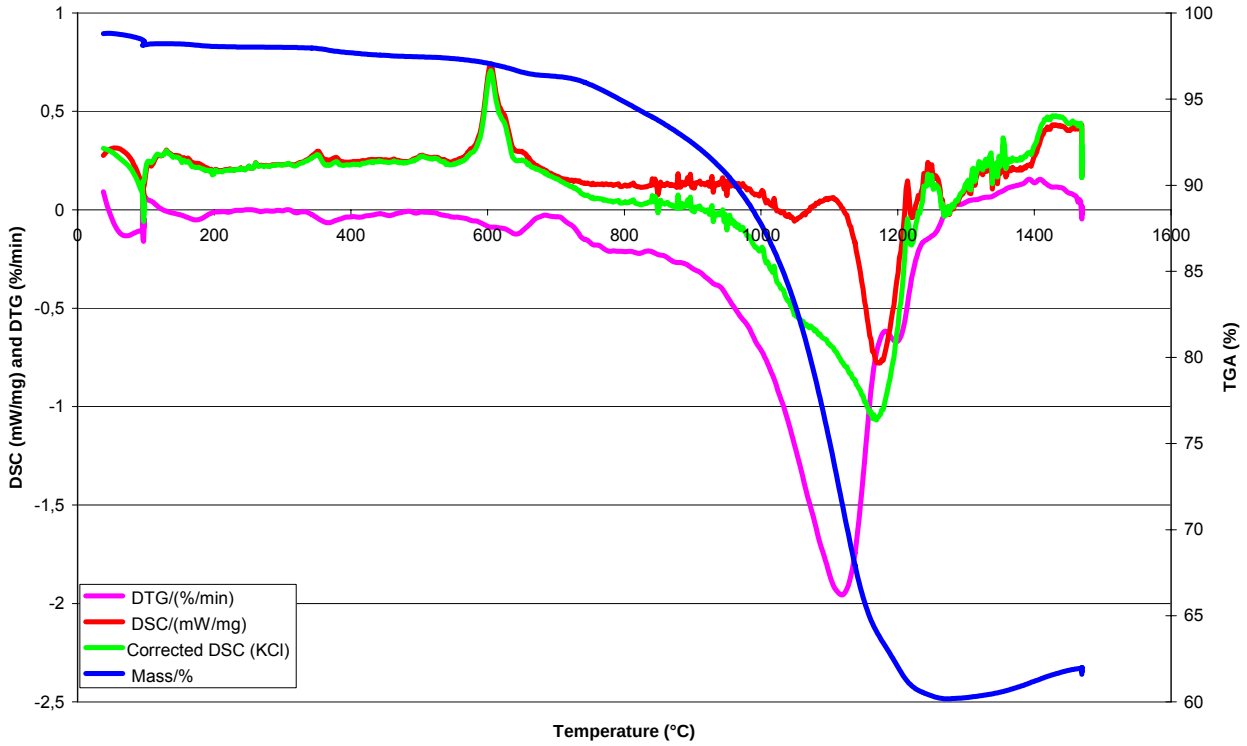

Figure 5-1: STA-diagram from the analysis of the ESP/E-filter ash from the Hjørring MSWI plant.

When these conditions are satisfied, the work of interpretation is complicated by some typical ash characteristics. Ash is a very composite material and several ash components may have similar evaporation temperatures. This makes the identification of the evaporating compound difficult and therefore makes it necessary in some cases to make use of an “average” evaporation enthalpy in order to quantify the melting, thereby introducing uncertainties.

In Figure 5-2, the melt curve based on the STA-output shown in Figure 8 is provided. This melt curve is proportional to an integration of the area between the corrected base line (green) and the solid black line in Figure 8. Notice that the melting goes on in two steps: First, 22 % (w/w) of the ash melt between 600 and 700 °C, which is then followed by a significant increase in the melt formation between 1200 and 1400 °C. We believe that the first melting is caused by inorganic salts, like chlorides and sulfates of the alkalies, and maybe some heavy metals, while the second phase on the melt curve is due to silicates melting.

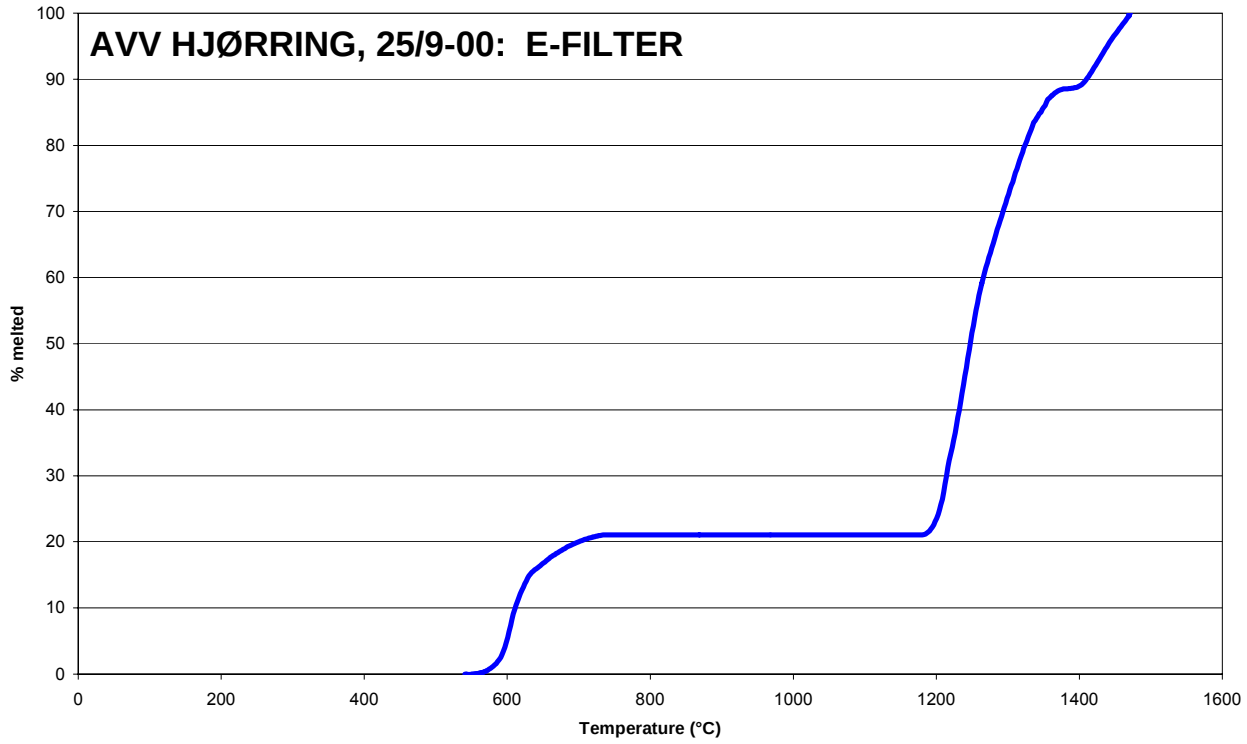

Figure 5-2: The melt curve for the Hjørring ESP/E-filter ash as calculated from STA-data. Notice that the melting goes on in at least two steps.

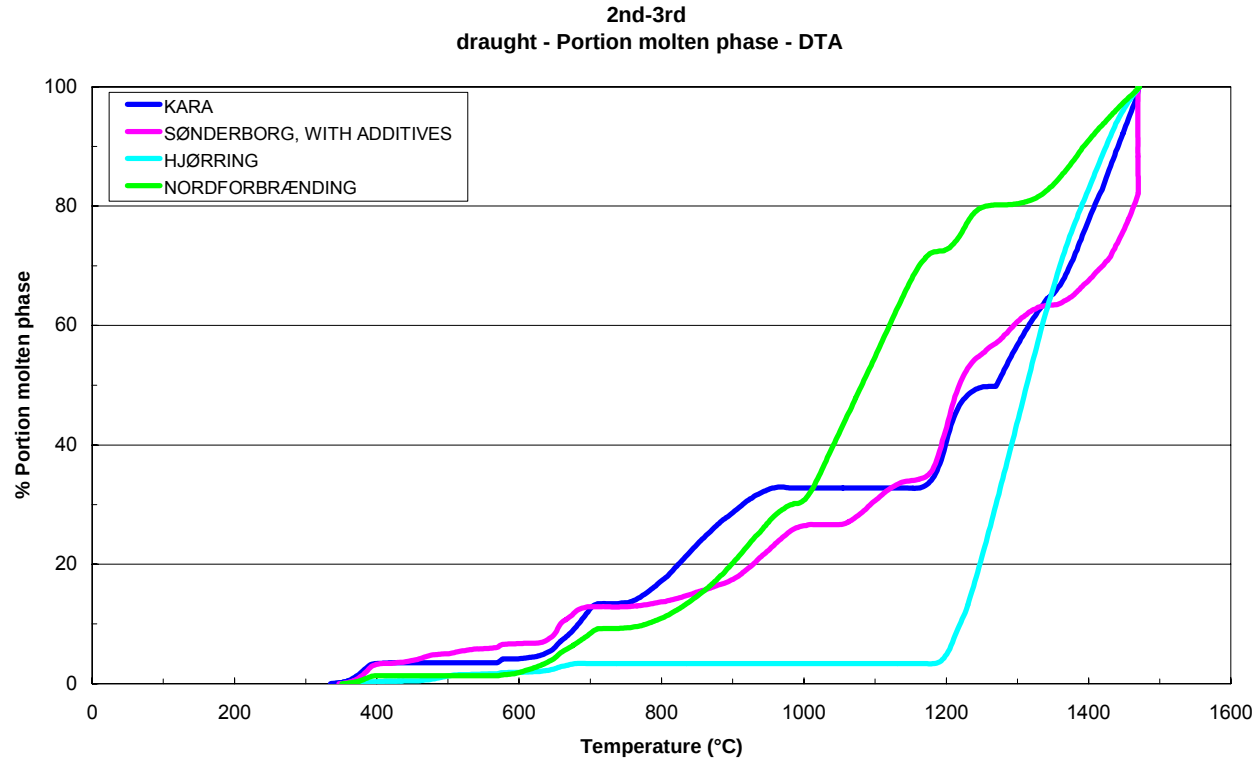

Figure 5-3: Melt curves for the 2nd-3rd Pass ash from each of the four plants investigated. The curves are calculated from STA-data. Notice that for all four plants the melting of the ESP/E-filter ash goes on in two steps.

In Figure 5-3, the melt curves for the 2nd-3rd Pass ash from all four MSWI plants are shown.

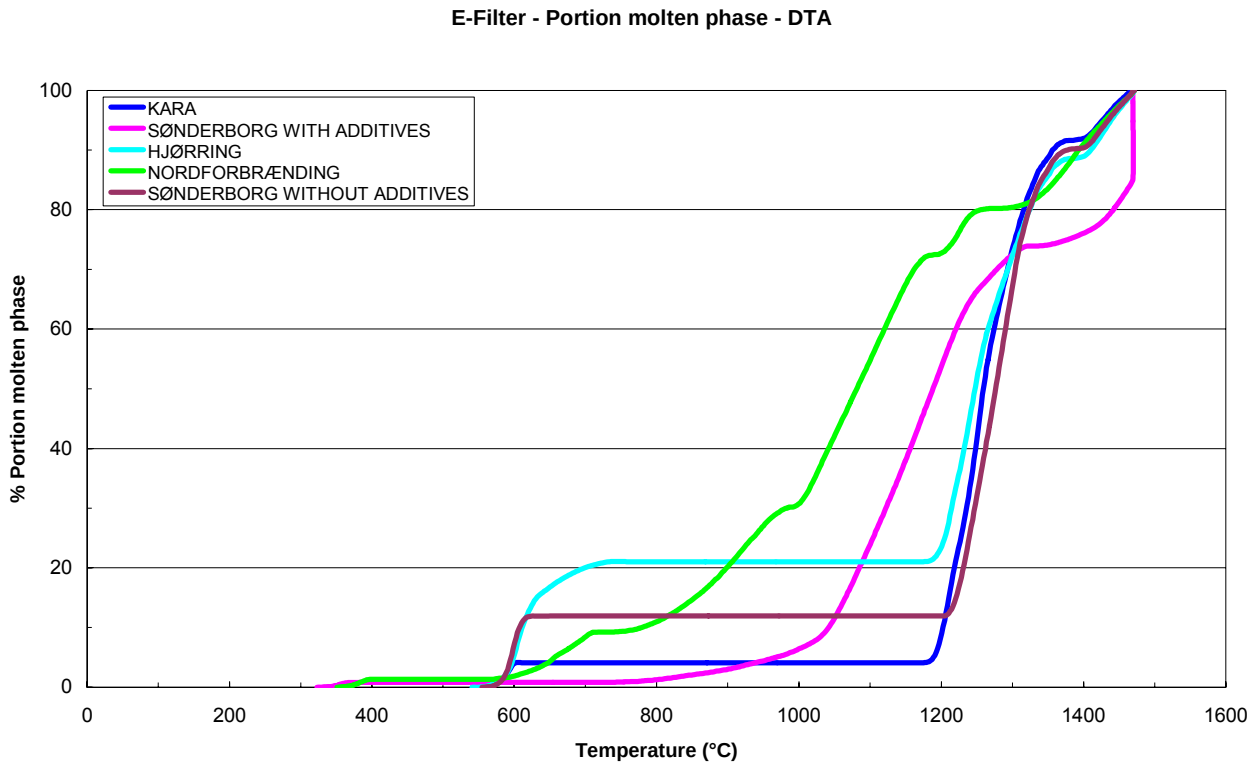

Figure 5-4: Melt curves for the ESP/E-filter ash from each of the four plants investigated. The curves are calculated from STA-data. Notice that for all four plants the melting of the ESP/E-filter ash goes on in two steps.

In Figure 5-4, the melt curves for the ESP/E-filter ash from all four MSWI plants are shown. For the Sønderborg (SKVV) plant two melt curves are shown, one corresponding to waste incineration without an additive, the other corresponding to waste incineration with an additive applied. It is noticed that all melt curves have two phases, corresponding to melting of simple salts and silicates. Furthermore, the additive applied at the Sønderborg (SKVV) MSWI plant – and aluminosilicate species - is seen to affect the melt progress of the ESP/E-filter ash significantly.

The identification of the peaks in the DSC curve is not straightforward. The energies associated with melting of ash are often quite low and distinct peaks are seldom observed. Moreover, in certain situations the DSC curve may have a drift (upward or downward) which makes it difficult to understand if and when the last melting peak is finished upon reaching of the highest temperature used in the experiments. The drift is probably mainly caused by different mass and thermo physical properties between sample and the reference material. Alternatively, the drift can be caused by the subtraction of an incorrect baseline.

Based on the work of Hansen et al. (1999) and due to the peculiar glass characteristics relevant particularly for bottom ashes (melting occurring over a wide range of temperature, no distinct melting enthalpy, possibility of devitrification, i.e. exothermic reactions), a series of experiments have been carried out in the STA in order to evaluate the reliability of the original analysis concept.

Based on these supplementary experiments, it can be concluded that, the application of STA for characterizing the melting of ashes, may be difficult, particularly if the ash has a glassy structure, for a number of reasons:

- The maximum temperature reached by the STA is 1500 ºC. At this temperature, some ash components may not be completely molten. The procedure typically used for the evaluation of the STA curves is based upon the assumption that the melting is 100%, at the end of the measurement. However, this assumption may not always be valid, particularly for ashes from coal or other materials containing high concentrations of silicon and aluminum, or for composite material formed by ash and sorbents, e.g. from investigations of alkali adsorption.
- In some cases, ash displays intense DSC-signals during heat-up. Often, this accompany evaporation or a phase change, rather than melting. When large quantities of ash vaporize there may be a significant influence of the choice of the evaporation energy on the melting curve, indicating the need to know the identity of the evaporating substances before proceeding with the analyses of the molten fraction.
- The melting enthalpies of glassy substances are very low. Melting of glass occurs over a wide range of temperatures and is not accompanied by a specific melting enthalpy as for crystalline substances. Melting enthalpies of glassy substances may be within the measurement error of the instrument. In this specific context, the measurement error includes uncertainties caused by changes in mass, heat capacity, and thermal conductivity, caused by evaporation and sintering of the sample.

It should be emphasized that not all ash has a glassy structure, and there are examples that show clear indications of beginning and end of a melting event. However, at present, our conclusion is that it is difficult to know in advance which ash samples will have a glassy structure. It may therefore be risky to assume *a priori* that the STA will be able to provide a quantification of the melting of Si-rich ashes, while for ashes rich in salts like ESP/E-filter ashes from thermal conversion of biomass or waste, the STA may provide a correct picture of the melting process.

Chapter 6:

Thermodynamic Considerations

By Flemming J. Frandsen, Lars Sørum, Mette K. Jensen, Rainer Backman

One of the big challenges in modern MSWI plants is the extreme variation in the quality of the incoming waste. By quality, we mean the chemical and physical composition of the incoming waste. It may, in principle, be possible to decrease the often seen significant corrosion in MSWI plants, caused by the formation of low-melting liquid phases of metal chlorides in the inner layers of deposits, if one can decrease the vaporization of these metal chlorides in the furnace. To investigate how this may be possible in a full-scale MSWI boiler is difficult and may be very expensive. Thus, we decided to adapt multi-phase, multi-component, global equilibrium analyses (GEAs), in order to deduce the effect of major elements on the vaporization of heavy metals like Cu, Pb and Zn, which are the main contributors to chemically aggressive metal chlorides in deposits.

In addition, an equilibrium model was applied to predict the melting behaviour measured for the 2nd – 3rd pass and ESP/E-filter ashes by STA and reported in Chapter 5 of this report.

6.1. GEA Model of a MSWI Plant

In order to understand the release of heavy metal species from burning waste, to quantify the re-condensation of those trace elements during cooling of the flue gas, and thereby to be able to decrease the mobility of heavy metals in MSWI plants, further knowledge on the behaviour of heavy metals in the combustion zone, and in the flue gas between the furnace and the flue gas cleaning devices, is needed.

Several studies using equilibrium calculations to investigate the fate of heavy metals in combustion systems have been reported in the literature. Equilibrium analyses have been applied for studying trace element partitioning in methane combustion (Wu et al. (1994)), waste combustion (Verhulst et al. (1996)), and in coal gasification and combustion processes (Frandsen et al. (1994)). Common for all these GEA studies is that no ash species have been included. The ash forming elements may react chemically with heavy metals, thereby forming e.g. silicates, aluminates or aluminosilicates, which will affect the volatilization, distribution and partitioning of these during thermal fuel conversion.

The objective of the present GEA model development has been to investigate the influence of varying operational parameters and MSW compositions on the release and chemical reactions of various heavy metals at typical combustion conditions in a grate furnace. Ash species have been included, in order to investigate possible reactions between these and the heavy metals. The main focus of the study has been on the influence of temperature, ash/metal ratios and the air/fuel ratio.

The program MINGTSYS minimizes total Gibbs free energy for a mass-balance constrained system of selected chemical species. Thermodynamic data were taken from GFE-DBASE, version 2.0. For further details on MINGTSYS and GFE-DBASE, please refer to Frandsen et al. (1994, 1996).

A comprehensive list of ash and trace element species was applied in the present model, including the heavy metals As, Cd, Cr, Cu, Hg, Ni, Pb, Zn, and the ash forming elements Al, Ca, Fe, and, Si. Other ash forming elements like, sodium (Na), potassium (K), and phosphorous (P) were not included in the original model although they may compete with the heavy metals on the access to sulphur (S) and chlorine (Cl). For a complete list of chemical species included, please refer to Sørum et al. (2003).

GEA has several limitations when applied on thermal fuel conversion systems. First and foremost, the residence time need to be long enough, or the temperature must be high enough, to ensure that all reactions reaches equilibrium. A turbulent flame or a similar flow system may introduce local conditions e.g. temperature or compositional gradients which are not taken into account in a GEA: the actual system modelled is considered as a box with a uniform temperature and chemical composition. Physical adsorption, chemisorption and capillary condensation phenomena are not taken into account either. Due to lack of appropriate solid and liquid phase mixing models for non-ideal behaviour, pure condensed phases and ideal gas was assumed in the original model (Sørum et al. (2003)). Finally, the mode and occurrence of a trace element in a particular fuel will affect the release of that trace element to the combustion gas in real live. This is not taken into account in GEA, where free access to all specified elements is assumed.

6.1.1. Release of Heavy Metals from the Grate.

A characteristic composition for MSW, consisting of 33,1 %(w/w) paper and cardboard, 6,5 %(w/w) plastics, 24,4 %(w/w) wet organic waste, 6,4 %(w/w) glass, 3,7 %(w/w) metals, 12,6 %(w/w) of other combustible materials (wood, rubber, leather, textiles), and a rest fraction of 13,3 %(w/w) (ash, sand, stones, fines, etc.), was used to calculate the elemental and heavy metal concentrations in the fuel. The result is shown in Table 6-1.

The conditions investigated in this study reflect those of a commercial grate-fired MSWI plant. Details on typical grate furnace and flue gas cleaning systems, was provided by Sørum et al. (1997). Calculations were performed in order to simulate the conditions on the grate, where both reducing and oxidizing zones exists, and in the flue gas duct, where there is an excess of oxygen. Thus, air excess numbers, defined as in Frandsen et al. (1994), in the range [0 - 0.9] and [1.2 – 1.9] were applied for the grate, while the air excess number in the flue gas duct was varied in the range [1.2 – 1.9].

MAJOR SPECIES:	COMPOSITION, %(W/W)	TRACE ELEMENTS:	CONCENTRATION [G/TON]
C	25.29	As	18.2
H	3.39	Cd	40.9
O	18.06	Cr	55.7
N	0.48	Cu	462.9
S	0.17	Hg	1.1
Cl	0.56	Ni	28.4
Moisture	24.82	Pb	136.0
Ash	27.24	Zn	1713.7

Table 6-1: Ultimate analysis of the characteristic MSW applied in this study.

Concerning the relevant temperature range, an adiabatic flame temperature of ~ 1500 K was calculated for the fuel composition provided in Table 6-1 and an air excess number of 1.9. Thus for the grate, it was decided to perform simulations covering the temperature range: [950 – 1600 K], while the cooling of the flue gas was studied in the temperature range [1600 - 300 K]. A temperature of 950 K is believed to correspond to total devolatilization of a waste-type fuel (Sørum et al. (2003)).

For a complete outline of the calculations performed with the model, please refer to Sørum et al. (2003, 2004). These two papers are provided in Appendices B-C of this report.

The main conclusion of the thermodynamic modelling of a MSW-fired incineration plant is that the elements cadmium (Cd), mercury (Hg), and lead (Pb), are fully vaporized on the grate. The elements arsenic (As), cupper (Cu), nickel (Ni), and zinc (Zn), is partly volatile. The element chromium (Cr) was shown to be stable in the condensed phase, mainly as solid Cr_2O_3, on the grate (Sørum et al. (2003)).

6.1.2. Partitioning of Heavy Metals during Cooling of the Flue Gas

Although a certain retainment of some the elements where calculated under grate firing conditions, a full access to all elements where assumed when doing the cooling profile thermodynamic calculations. All the elements, except mercury (Hg) were shown to re-condense on the surface of fly ash particles in the flue gas during cooling in the flue gas duct (Sørum et al. (2004)).

6.1.3. Effect of Fuel Feedstock on Heavy Metal Release

The model developed by Sørum et al. (2003, 2004) was extended and applied in a subsequent study to predict the effect of the fuel feedstock mixture on the release of the heavy metals, Cu, Pb and Zn. The extension was the application of mixing models, and taking into account also the alkalies, i.e. sodium (Na) and potassium (K).

The baseline composition of the considered MSW was changed in order to investigate the effect of the fuel feedstock composition on, the release og Cu, Pb, and Zn. All three metals are suspected of being main carriers of chlorine from the grate zone to the heat transfer surfaces in the superheater and subsequent boiler sections. The **molar** ratios: Al/Me, Ca/Me, Si/Me, Cl/Me and S/Me were all changed - one at a time - between the values {1, 5, 10, 100}, where Me $\in$ {Cu, Pb, Zn}. The calculations were done, using the commercial Gibbs free energy minimizer, FactSage, Version 5.2. For the pure condensed and gaseous phases of the trace elements, thermochemical data from GFE-DBASE, Version 2.0, were transformed to FactSage format and applied.

Below is an outline of the results obtained.

Al/Me – ratio:

The volatility of the elements Cu and Zn was only slightly affected by the Al/Me-ratio. For cupper, Cu, a higher volatility was observed when changing the Al/Cu-ratio, particularly from 25 to 100. For zinc, the highest volatility was observed at Al/Zn = 25, while an even further increase in the molar ratio between Al and Zn caused a decrease in the volatility of Zn, most likely due to formation of zinc aluminates, $ZnO.Al_2O_3$. Lead, Pb, showed no significant effect to be caused by a change in the Al/Pb-ratio. In Figure 6-1, the molar fraction of Zn released to the gas phase for various Al/Zn-ratios is shown as a function of temperature.

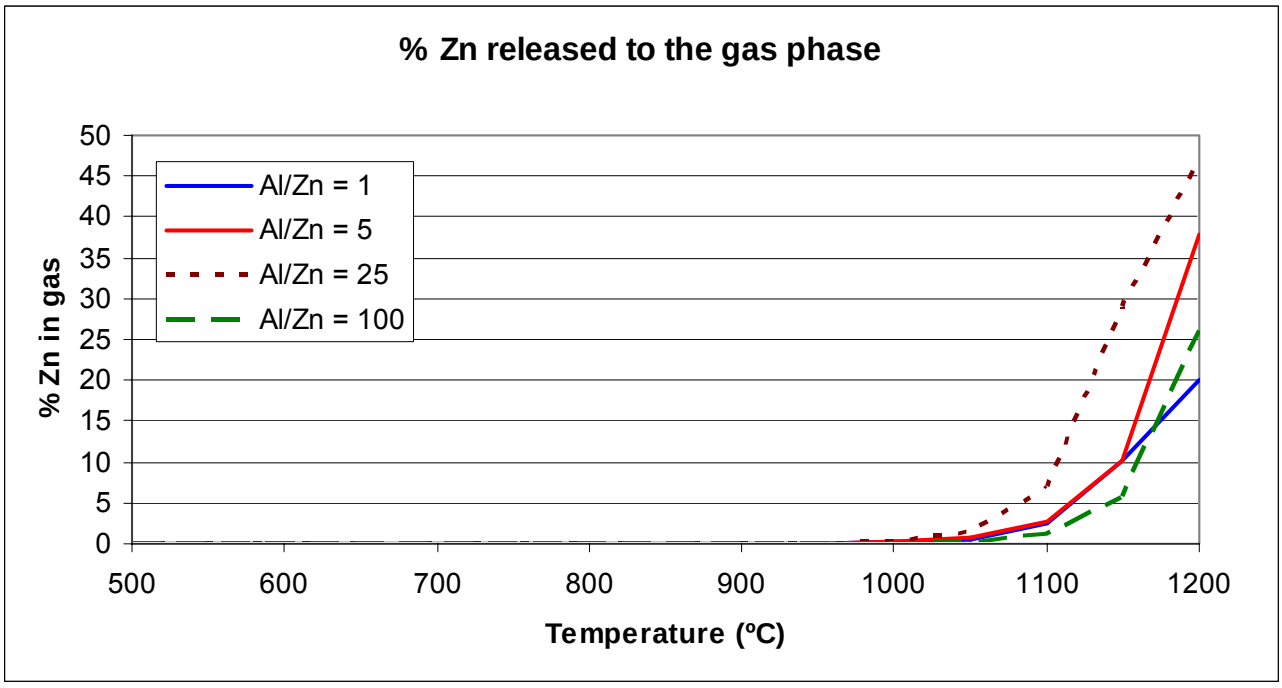

Figure 6-1: The molar fraction of Zn released to the gas phase for various Al/Zn-ratios is shown as a function of temperature. Notice that the temperature is shown in [°C]. Actual air excess number: $\lambda = 1.5$.

Ca/Me – ratio:

As for the Al/Me-ratio, only Cu and Zn are affected by a change in the Ca/Me-ratio. Zinc is affected in the same way as described for the Al/Zn-ratio. For Cu, a low ratio of the Ca/Cu-ratio seems to enhance the volatilization of Cu. For high Ca/Cu-ratios an increase in the volatility of Cu is observed (compared to lower Ca/Cu-ratios). Lead, Pb, is not affected at all by a change in the Ca/Pb-ratio.

In Figure 6-2, the molar fraction of Cu released to the gas phase for various Ca/Cu-ratios is shown as a function of temperature.

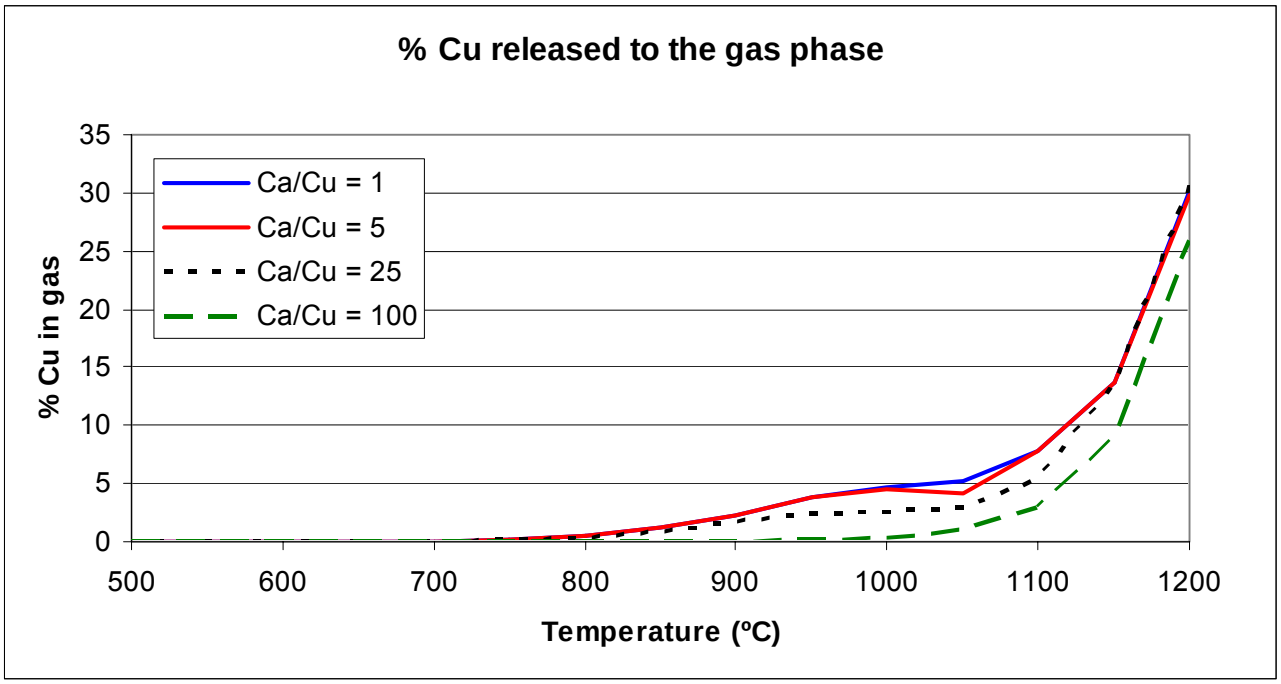

Figure 6-2: The molar fraction of Cu released to the gas phase for various Ca/Cu-ratios is shown as a function of temperature. Notice that the temperature is shown in [°C]. Actual air excess number: λ = 1.5.

Si/Me –ratio:

Silicon has a pronounced effect on the volatility. For all three elements, an increase in the amount of metal volatilized, is observed with an increasing Si/Me-ratio.

This significant effect of silicon may be explained by the fact that an increased amount of Si in the system will affect the Ca-Si – chemistry, simply by causing increased formation of Ca silicates at the expense of $CaCl_2$ (cr), which will release a significant amount of Cl, known to make heavy metals highly volatile.

In Figure 6-3, the molar fraction of Pb released to the gas phase for various Si/Pb-ratios is shown as a function of temperature.

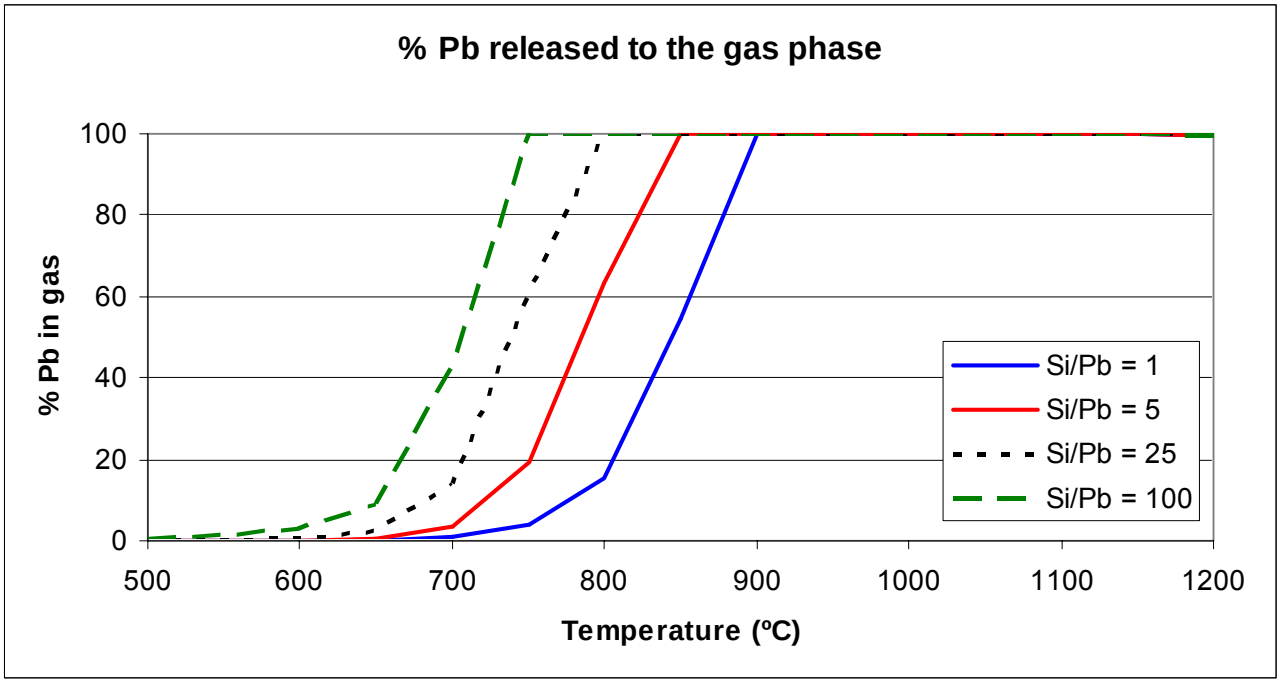

Figure 6-3: The molar fraction of Pb released to the gas phase for various Si/Pb-ratios is shown as a function of temperature. Notice that the temperature is shown in [°C]. Actual air excess number: λ = 1.5.

Cl/Me – ratio:

Chlorine makes all three metals more volatile, mainly due to increased formation of volatile Me-chlorides when increasing the Cl/Me-ratio.

In Figure 6-4, the molar fraction of Cu released to the gas phase for various Cl/Cu-ratios is shown as a function of temperature. It is seen that the Cl/Cu-ratio has a significant effect on the fraction of Cu volatilized. At 900 °C 60 % on a molar base of the Cu is vaporized at Cl/Cu = 100, while < 1 % is released at Cl/Cu = 1 (and Cu does indeed form a volatile cupper(I)-chloride, CuCl(g)).

S/Me – ratio:

The S/Me-ratio has the same effect on the volatility as was reported for the Cl/Me-ratio. This may at first sight be a bit surprising, but may be explained indirectly. All three metals form stable sulfatic compounds, but when adding huge amounts of sulphur to the system, a lot of the Ca being present is sulphated, thereby releasing significant amounts of chlorine, which is thermodynamically available for reactions with e.g. heavy metals, thereby causing increased volatility of these.

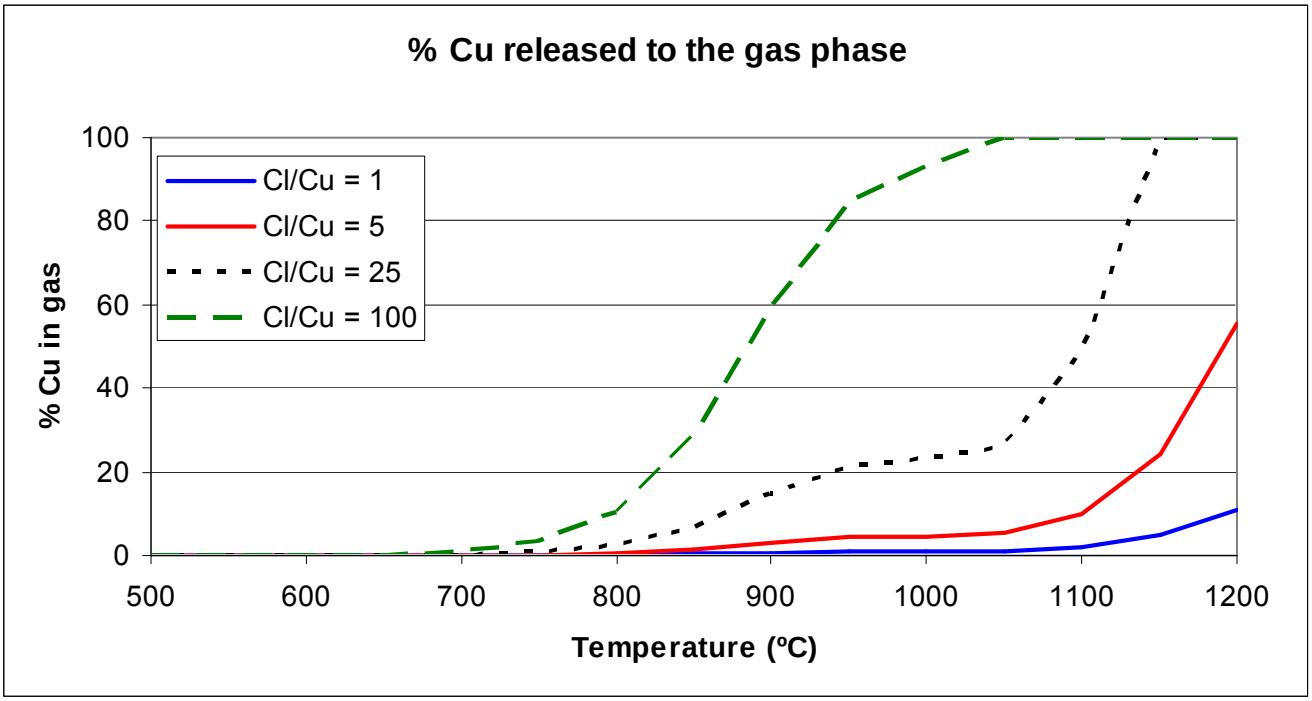

Figure 6-4: The molar fraction of Cu released to the gas phase for various Cl/Cu-ratios is shown as a function of temperature. Notice that the temperature is shown in [°C]. Actual air excess number: λ = 1.5.

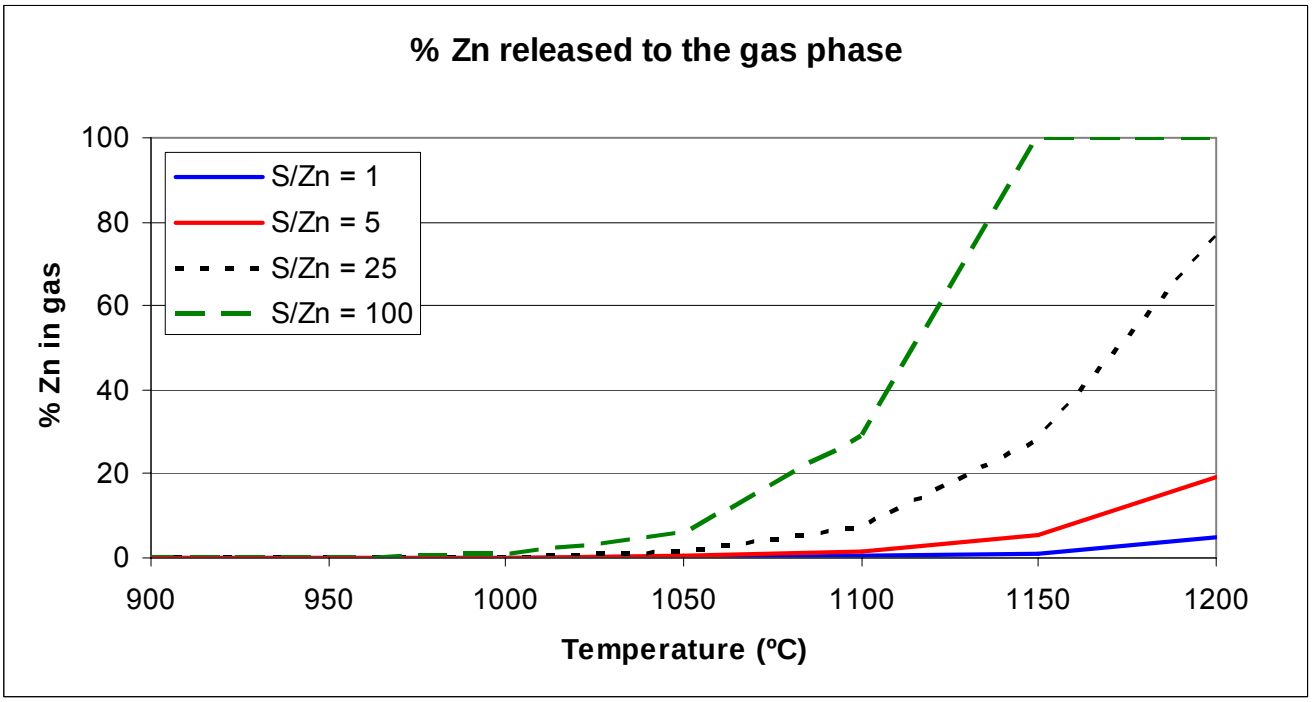

Figure 6-5: The molar fraction of Zn released to the gas phase for various S/Zn-ratios is shown as a function of temperature. Notice that the temperature is shown in [°C]. Actual air excess number: λ = 1.5.

In Figure 6-5, the molar fraction of Zn released to the gas phase for various S/Zn-ratios is shown as a function of temperature.

6.2. Prediction of Melting of MSWI Ashes

The commercially available Gibbs free energy minimizer, FactSage, Version 5.2., was also applied to predict the melting curves determined experimentally by Simultaneous Thermal Analysis (STA), see Chapter 5 of this report.

In Figure 6-6, the calculated meting of the 2nd-3rd Pass ashes from the four MSWI plants investigated is shown.

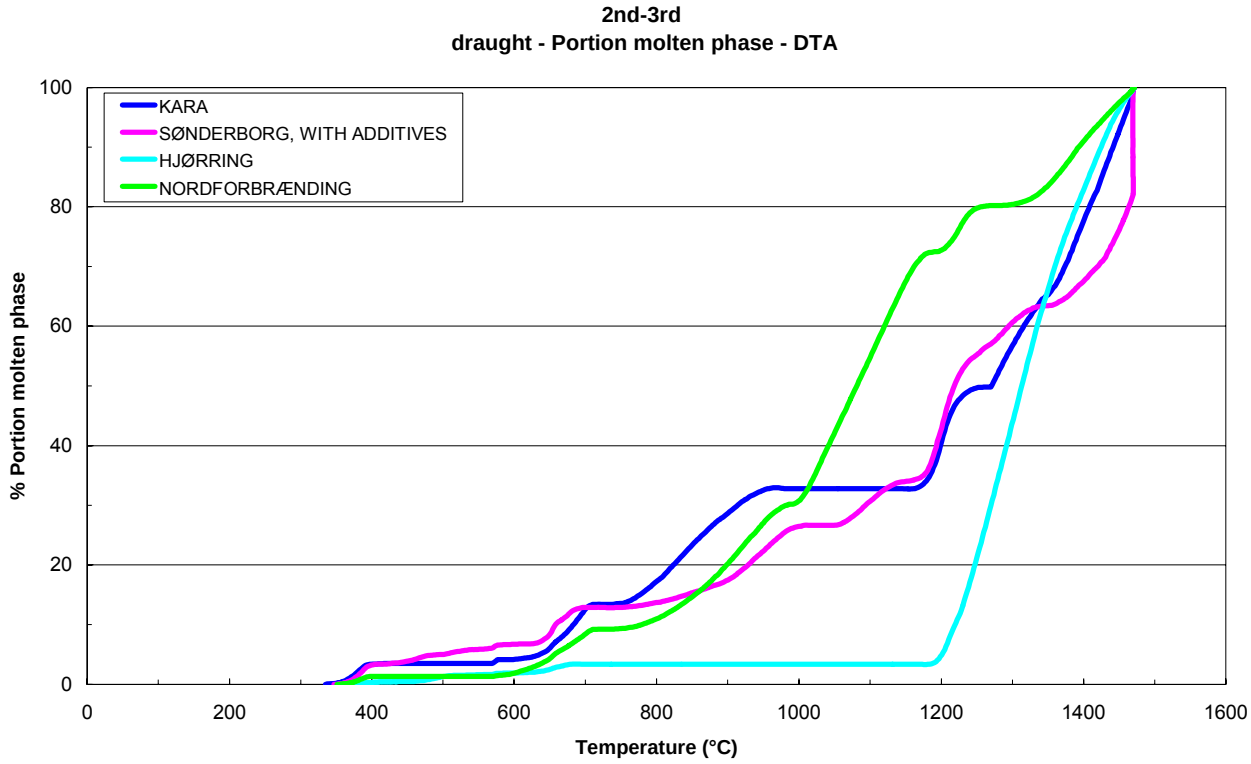

Figure 6-6: Calculated melting behaviour of 2nd-3rd Pass ashes from the four MSWI plants investigated in this project. This calculated behaviour may be compared to the measured melting behaviour shown in Figure 5-3.

In a similar way, the melting behaviour of the E-Filter/ESP ashes from the four plants was calculated by use of FactSage, 5.2. The result is shown in Figure 6-7.

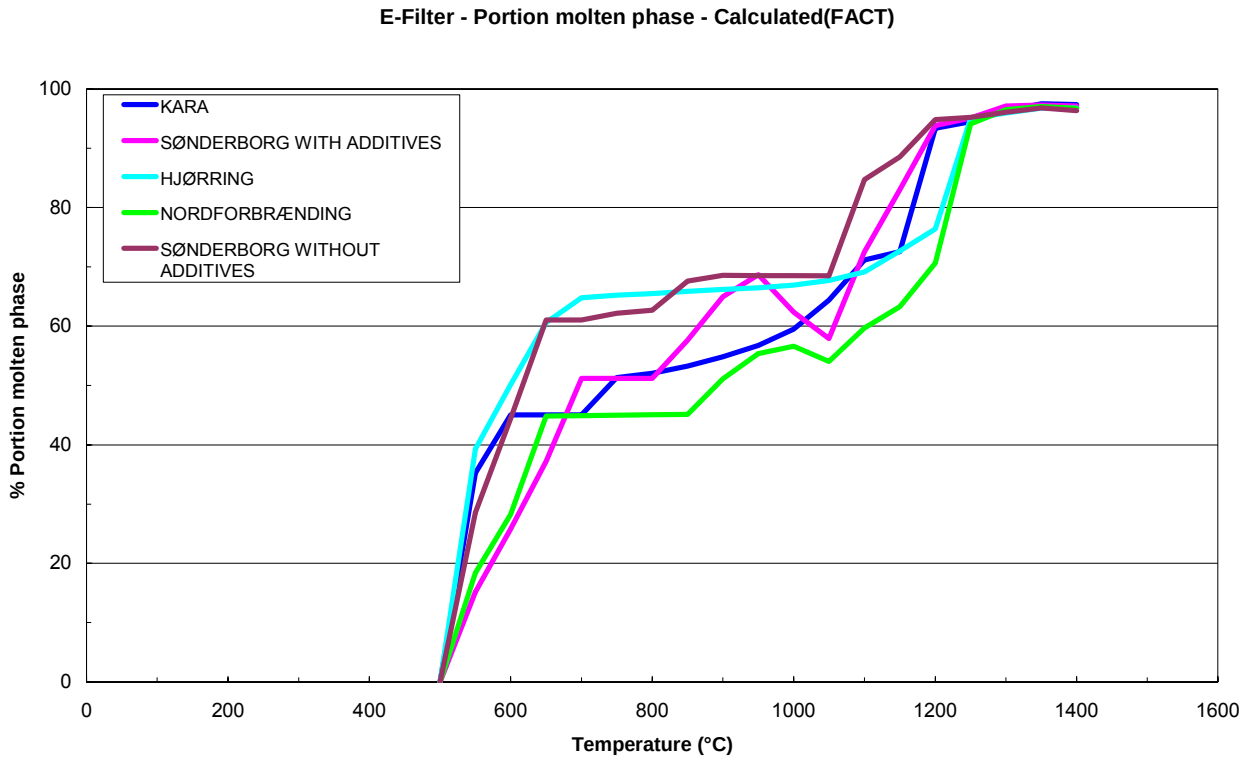

Figure 6-7: Calculated melting behaviour of E-filter/ESP ashes from the four MSWI plants investigated in this project. This calculated behaviour may be compared to the measured melting behaviour shown in Figure 5-4.

Extreme care must be taken when comparing Figure 6-6 directly to Figure 5-3, respectively Figure 6-7 directly to Figure 5-4. The figures are not directly comparable, and the idea has never been to reproduce Figures 5-3 – 5-4, theoretically by use of an equilibrium model. Instead the idea is to use the equilibrium model to interpret the measured melting behaviour of the different ashes.

The main difference between the applied equilibrium model and the measurements of melting reported in Chapter 5 is that the experiments goes on in flow system, i.e. an inert gas, N_2, flows through the system and will carry away volatile species being released from the investigated ash as the temperature of the samples increases. The applied GEA model simulates a batch system, i.e. a certain amount of gas is brought into contact with an ash with a specified chemical composition, and the volatilization of ash species and melting of the ash is calculated. Although the amount of gas in contact with the ash is determined based on the total duration of the experiment and data on the flow of gas, the two cases are still not directly comparable, due to the gradual change in the chemical composition of the ash in the experiment.

In Figure 6-8, the total weight loss of each of the ash samples investigated by the STA is shown. It is clear from the figure that some of the ash samples losses a significant amount of mass, by evaporation of volatile metal species.

Figure 6-8: The total loss of mass of each ash samples investigated by the STA vs. the temperature of the sample. E means ESP/E-Filter ash, while D means draught/2nd -3rd pass ash. K – KARA, H – Hjørring, N – Nordforbrænding, and S – Sønderborg. The +/- -signs refer to the presence or absence of an additive (only valid for the Sønderborg MSWI Plant). It is seen that the ESP/E-filter ash from the additive experiments at Sønderborg looses 80 % of its mass due to evaporation of volatile metal species.

Although there a serious limitations in the GEA model applied when it comes to calculating the melting behaviour of the ashes, there are some interesting features to be seen. First, also the theoretical melting curves reveal at least a 2-step melting, in some cases even multi-step melting of the ashes. The same observation was made for the experimental curves shown in Chapter 5.

The chemical composition of each of the ash samples investigated in the STA was calculated by use of the GEA model applied. A temperature of 1100 °C was assumed for the 2nd-3rd pass ashes, while the composition was assumed to be frozen at 500 °C for the ESP/E-filter ashes. The result is shown in Figure 6-9, where the chemical composition is grouped into categories: AlkSalt, CaSalt and Oxides. AlkSalt covers the sum of the content of the alkali salts: KCl, NaCl, and K_2SO_4. CaSalt covers the sum of the content of the calcium salts: $CaSO_4$ and $Ca_3(PO_4)_2$. And Oxides covers the sum of the content of the oxides: CaO, ZnO, SiO_2, Al_2O_3, PbO, MgO, Fe_2O_3, and CuO.

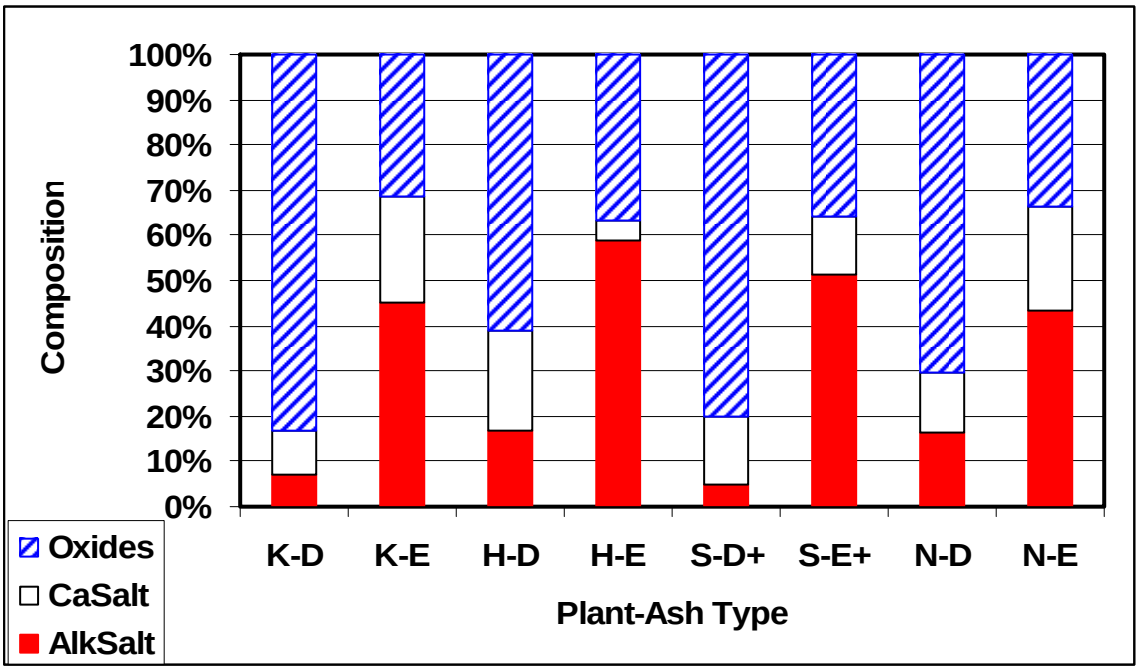

Figure 6-9: Calculated chemical composition of the different ashes investigated in this project. E means ESP/E-Filter ash, while D means draught/2nd -3rd pass ash. K – KARA, H – Hjørring, N – Nordforbrænding, and S – Sønderborg. The +/- - signs refer to the presence or absence of an additive (only valid for the Sønderborg MSWI Plant).

On Figure 6-9, it is seen that the content of oxides is significantly higher in the 2nd-3rd pass ashes compared to the ESP/E-filter ashes. This is the reason for the somewhat lower amount of melt formation predicted below 1000 °C for the 2nd-3rd pass ashes in Figure 6-6, compared to the ESP/E-filter ashes shown in Figure 6-7. Above 1000 °C, the oxides melt. At low temperatures, i.e. below 1000 °C, the multi-steps seen on Figures 6-6 – 6-7, is probably due to different salt fractions, e.g. chlorides, sulphates, and phosphates melting.

Further – future – experiments on synthetic mixtures are needed to address this in details.

Chapter 7:

Heat Transfer in Ash Deposits

By Flemming J. Frandsen and Ana Zbogar

The objective of this part of the actual project was to review the present knowledge about the heat transfer to and through ash deposits formed in utility boilers, and to propose the models for practical application e.g. heat transfer calculations. This is an issue of common interest, not only for MSWI Plants, but for all types of thermal fuel conversion systems.

Heat transfer will govern the deposit's surface temperature, thus influencing the conditions at the deposit surface i.e. if the surface is molten. Deposit surface conditions influence both the deposit build-up and removal: molten deposit may lead to a more efficient particle capturing, but also molten slag may flow down the heat transfer surfaces. Also, heat transfer characteristics will govern the temperature gradient inside the deposit, thus potentially causing shedding due to thermal shock between the deposit layers.

The main heat transfer parameters of interest are the convective heat transfer coefficient h, the thermal conductivity of deposit k, and the deposit's surface emissivity ε. The former is a function of flow characteristics, and can be calculated using different correlation equations. The latter two parameters depend on the deposit properties, and can be calculated using different structure-connected models.

The thermal conductivity of ash deposits, which has a porous structure, can be modelled using different thermal conductivity models for packed beds. Models can be divided into two major groups, by the way they treat radiation heat transfer i.e. the unit cell models and the pseudo homogeneous models. Which model will be suitable for a particular application depends primarily on the deposit structure i.e. whether deposit is particulate, sintered or fused.

As a part of this work, simple calculation of heat resistances for deposit on superheater tube was performed, showing that major resistances are in the heat transfer to the deposit and the heat conduction through the deposit. Very few experimental data for thermal conductivity of ash deposits, especially at high temperatures where radiation is important, are found in the literature. Although the structure of the deposit is essential for its thermal conductivity, most of the measurements were done on crushed samples. Results obtained using different models were compared with the experimental data published in Rezaei et al., measured on crushed coal ash samples. Although errors of the predictions were very high in most cases, two models were proposed as suitable for

heat conductivity calculations i.e. the Yagi and Kunii model for particulate deposits, and the Hadley model for sintered and fused deposits.

It was found that the major factor that influences the thermal conductivity of ash deposit is deposit state i.e. if the deposit is particulate, sintered or fused. Different models were tested using experimental results for two coal ash samples, obtained by Rezaei et al. It was found that simple structure models don't give satisfactory results for both non-sintered and sintered samples. Particulate deposits can be modeled using the Yagi and Kuni semi-empirical model, while sintered deposits should be modeled using the Hadley complex structure model. Experimental values for fused deposits were not available, but the suggestion is that they can also be modeled as sintered deposits, using the Hadley model. Finally, it can be concluded that a wide range of thermal conductivity models exist, but the need exists for a wide range of experimental data, which would help in evaluating these models. Also, it is necessary to formulate a more accurate model for thermal conductivity of solid mixtures, which is the property that can be identified as a potential important source of errors.

A review paper on heat transfer in deposits and models for all relevant sub processes, has been written and submitted for publication in Progress in Energy and Combustion Science. The paper is provided in Appendix D.

Chapter 8:

Summary and Conclusions

By Flemming J. Frandsen

The summary and conclusion provided in this Chapter is based on the content of this report, spiced up with information gained in two M.Sc.-Projects carried out within the frame of the project, Pedersen (2002) and Rasmussen (2004). In additions aspects of a review on current and future research challenges within ash and deposit formation in MSWI plants, provided by Dr. Flemming Frandsen, at the 23rd Ann. Int. Conf. on Incineration and Thermal Treatment Technologies, May 10-15, Phoenix, AZ, USA, have been included.

In the flame zone of a MSWI plant, a fly ash fraction, rich in Al, Ca, Fe and Si, is formed on the grate. Some of the ash is lifted from the burning fuel-bed and entrained with the flue gas through the flue gas channel. At the same time, the flame-volatile elements like Na, K, Zn, Pb, Cl and S are released - partly or fully - to the gas phase in the furnace. These elements form sulphates and chlorides which upon entrance to the convective pass, i.e. when the flue gas enters the superheater sections starts to condense heterogeneously on the surface of fly ash particles, thereby causing and increase in the concentration of these elements in the ESP/E-filter ash, at the expense of the non-volatile elements, Al, Ca, Fe, and Si. This pattern has been seen on all four plants investigated in this study. Thus, we have a good feeling and understanding of the chemistry going on in the plant. Anyhow, there is a serious lack of data on the physical ash formation process, i.e. how is the ash actually formed during heat-up, pyrolysis, and subsequent char burnout in the plant ? More detailed research is need on this in order to be able to quantify the particle size distribution development during MSW incineration on a grate.

From an analytical point-of-view, this study has shown a couple of interesting features:

- We did not identify any Pb- and Zn-containing salt phases by use of QXRD. This is a bit surprising since we expect the Pb and Zn to be released in the flame zone and then later on - upon cooling of the gas in the convective pass of the boiler – to recondense on the surface of fly ash particles as a simple salt, most likely chlorides or sulphates. The results obtained here seem to indicate that lead and zinc is rather present as oxides, probably in close contact with silicates. We will investigate this further in the near future, by doing advanced surface chemistry analyses of these ashes.
- A 1st generation CCSEM chemistry classification scheme for MSW-derived ashes, has been developed and tested, but it still needs further improvement, in order to keep the amount of ‘unclassified’ spots in the EDX-analyses at a reasonable low level. Furthermore, we want to modify the CCSEM chemistry classification to be applicable also for SEMPC (Point Count) analyses of deposits. This is also a future task to be solved.
- The STA analysis has shown its applicability within this study, but much further work is needed to make the transformation of the STA-output into a melt curve smooth and easy. A standardized identification of evaporation or melting peaks

would be nice to have. We are currently trying to simulate the measured melting of the actual ash samples by use of multi-component, multi-phase thermodynamic equilibrium calculations. The aim is to identify the chemistry behind the two phase melting curves shown in this report.

An analytical tool for characterization of the behaviour of ashes in MSWI plants which was not reported here is the TOF-SIMS surface characterization, which will identify the chemistry on the surface of fly ash particles. We will apply both techniques and will correlate them with the other techniques some time in the near future.

A significant number of thermodynamic modelling activities have conducted as part of this project:

- First, a two-chamber model was developed and applied to predict trace element release from the grate and recondensation during the subsequent cooling of the flue gas between the furnace and the particulate removal filter. This study revealed that not all trace elements are fully volatile under grate-firing conditions, in case the thermodynamic equilibrium is valid in this zone. Most of the elements, with exception of mercury, Hg, are recondensed during cooling of the flue gas.
- Secondly, a parametric study was conducted in order to investigate the effect of the feedstock chemical composition on the release of volatile heavy metals. This study showed that addition and thereby direct intimate contact on the grate of certain ash forming elements like Si, S and Cl, is something that must be done with extreme caution. Our simulations indicated for example that addition of Si to a baseline feedstock composition will cause reaction with Ca in the mixture, thereby releasing significant amounts of Cl, which will cause an increased volatilization of certain heavy metals, like Cu, Pb and Zn.
- Finally, we have adapted a thermodynamic model in order to interpret the experimentally determined melting curves from a number of 2^{nd}-3^{rd} pass and ESP/E-filter ashes. The thermodynamic model, although being limited by a number of assumptions, proved very useful in interpreting STA-melting data.

The last part of the project dealt with heat transfer through deposits. This is an issue of common interest when working with deposit formation in utility boilers fired with all types of fuels, not only MSW. The main heat transfer mechanism inside deposits is heat conduction. The trick is to be able to calculate an effective thermal conductivity, in order to be able to quantify the amount of heat being transferred through a deposit. This is relevant when trying to estimate the surface temperature of deposits and when designing boilers (when calculating the heat-uptake profile in the boiler). The conclusion is that several models are available, but extreme care must be taken when choosing a model for this purpose. The outcome of this model review will in the future be implemented in software for prediction deposit build-up, consolidation and shedding.

Acknowledgment:

This work was carried out as part of the CHEC Research Centre at the Department of Chemical Engineering, Technical University of Denmark. The CHEC Research Centre are financially supported by Energy E2, Elsam, The Danish and Nordic Energy Research Programmes, The Danish Technical Research Council and the European Union. The authors are especially thankful to EFP Proj. J. No. 1373/01-0029 for funding of this particular work.

Also a thank is given to the Institute for Environmental Science and Engineering at the Center for Advanced Research on Ecomaterials (CARE), Nanyang University of Technology, where Dr. Laursen performed the XRD-work reported here.

To the crew at the Centre for Applied Surface and Micro Analysis, especially, Leif Højslet, Pia Wahlberg and Dorthe Larsen, goes special acknowledgment for several hours at the SEM and several GBytes of high-quality digital images belonging to the world of ash and deposit formation … and corrosion.

Finally a special and very warm thanks to Bengt-Johan Skrifvars and Rainer Backman at

the Åbo Akademi University for several hours of deeply inspiring discussions on these

things ……

References:

Bryers, R. W. (1996): Fireside slagging, fouling, and high-temperature corrosion of heat-transfer surface due to impurities in steam-raising fuels. *Prog. Energy Combust. Sci.* 22 (1996) pp. 29-120

Cheary and Coelho (1992): A fundamental parameters approach to x-ray line fitting. *J. Appl. Cryst.*, 25 (1992) pp. 109-121.

Frandsen et al. (1994): Trace Elements from Combustion and Gasification of Coal - An Equilibrium Approach. Prog. Energy and Comb. Sci. 20(1994) pp. 115-138.

Frandsen et al. (1996): GFE-DBASE - A Pure Component Trace Element Thermochemical Database. CALPHAD 20(2) 1996 pp. 175 – 229.

Hansen et al. (1999): Quantification of Fusion in Ashes from Solid Fuel Combustion. *Thermo-chimica Acta*, 326 (1999) pp. 105 – 117.

International Ash Working Group (IAWG) (1997): Municipal Solid Waste Incinerator residues. *Studies in Environmental Science 67*, Elsevier, 1997

Laursen, K. (1997): Characterization of Minerals in Coal and Interpretations of Ash Formation and Deposition in Pulverized Coal Fired Boilers, Geological Survey of Denmark and Greenland, Ph.D.-Thesis, ISBN-87-7871-022-7.

Pedersen, R. S. (2002): Advanced Characterization of Municipal Solid Waste Ashes. M.Sc.-Project Final Report, CHEC Research Centre, Department of Chemical Engineering, DTU, 2002.

Rasmussen, A. E. (2004): Waste Incineration. M.Sc.-Project Final Report, CHEC Research Centre, Department of Chemical Engineering, DTU, 2004.

Statistisk Årbog (2000): Danmarks Statistik, November 2000, ISBN-87-501-1125-6.

Sørensen (1999): Computer Controlled Scanning Electron Microscopy (CCSEM) Analysis of Straw Ash *Proc. Eng. Found. Conf. 'Impact of Mineral Impurities in Solid Fuel Combustion'*, Kona, Hawaii, November 2-7, 1997.

Sørum et al. (1997): Heavy Metal Partitioning in a Municipal Solid Waste Incinerator. Proc. 5th Annual North American Waste-to-Energy Conf. April 22-25, 1997, Raleigh, NC, USA.

Sørum et al. (2003): On the fate of heavy metals in municipal solid waste combustion. Part I: Devolatilization of heavy metals on the grate. Fuel 82 (2003) pp. 2273 – 2283.

Sørum et al. (2004): On the fate of heavy metals in municipal solid waste combustion. Part II: From furnace to filter. Fuel 83 (2004) pp. 1703 – 1710.

Verhulst et al. (1996): Thermodynamic Behaviour of Metal Chlorides and Sulphates under the Conditions of Incineration Furnaces. Env. Sci. Techn. 30(1996) pp. 50 – 56.

Wu et al. (1994): A model to assess heavy metal emission from municipal solid waste incineration. J. Hazardous Waste and Hazardous Materials 11(1) 1994 pp. 71 – 92.